ESCUELA TÉCNICA SUPERIOR DE INGENIERÍA DE TELECOMUNICACIÓN

UNIVERSIDAD POLITÉCNICA DE CARTAGENA

Proyecto Fin de Carrera

Análisis y Diseño de Antenas Planas de Alta Ganancia

AUTOR: Cristina Arias Pérez
DIRECTORES: Dr. José Luis Gómez Tornero
Dr. Alexandros Feresidis
(Universidad de Loughborough, Inglaterra)

Cartagena, Julio de 2007

Autor	Cristina Arias Pérez
E-mail del Autor	cristinarias@hotmail.com
Director(es)	José Luis Gómez Tornero, Alexandros Feresidis
E-mail del Director	josel.gomez@upct.es, A.Feresidis@lboro.ac.uk
Codirector(es)	
Título del PFC	Análisis y Diseño de Antenas Planas de Alta Ganancia
Descriptores	Superficies Selectivas en Frecuencia (FSS), Estructuras periódicas, Antenas Leaky-Wave, Antenas Surface-Wave

Resumen

En este proyecto, se ha desarrollado un análisis basado en la aplicación de la Técnica de Resonancia Transversa con el objetivo de obtener el Diagrama de Dispersión y Diagrama de Radiación de antenas compuestas por Superficies Selectivas en Frecuencia (FSS). Se han estudiado tres estructuras distintas con una característica en común: todas están compuestas por superficies periódicas de parches formadas por dipolos o tripolos pero actuando según diferentes modos de operación, según se comporten como antenas Surface-Wave o Leaky-Wave. La técnica implementada se ha verificado mediante resultados encontrados en distintos artículos y medidas reales realizadas en anteriores experimentos. La solución eficiente y rápida que presenta este método se ha visto como una ventaja sobre otras técnicas como puede ser la realización de un análisis modal sobre toda la estructura.

Titulación	Ingeniero de Telecomunicación
Intensificación	Sistemas y Redes de Telecomunicación
Departamento	Tecnología de la Información y las Comunicaciones
Fecha de Presentación	Julio de 2007

ÍNDICE

PARTE I

PARTE II

Análisis y Diseño de Antenas Planas de Alta Ganancia

TABLA DE CONTENIDOS

1 Introducción

Las Superficies Selectivas en Frecuencia (Frequency Selective Surfaces, FSS), estructuras conocidas por su uso como filtros de microondas y de señales ópticas, constituyen la base de este proyecto. Estas superficies consisten en estructuras periódicas, representadas a través de diferentes formas y distribuciones, y tienen múltiple aplicaciones como antenas mejoradas para nuevos sistemas de comunicación inalámbrica y en general en ingeniería de microondas, obtenidas con bajo coste y simple fabricación.

Con estructuras periódicas, se refiere a infinitas líneas de transmisión o guías de onda cargadas a intervalos periódicos con idénticos elementos reactivos. Éstos pueden ser parches metálicos o aperturas en una pantalla metálica y muestran reflexión total (parches) o transmisión total (aperturas) a determinadas frecuencias. Existen varios tipos de estructuras periódicas y se diferencian principalmente en la forma de los elementos reactivos o en la distribución de éstos sobre la superficie, pero todos estos casos se pueden modelar con reactancias dispuestas en paralelo a través de una línea de transmisión como la que se muestra en la *Figura 1*.
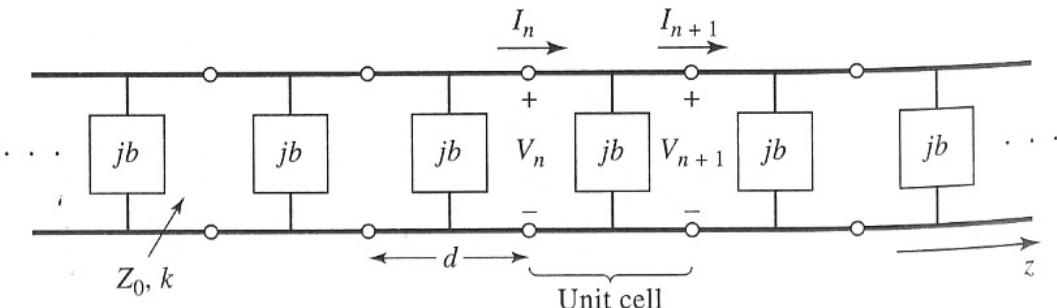
Figura 1. Circuito equivalente de una línea de transmisión cargada periódicamente. La línea tiene una impedancia característica Z_0 y una constante de propagación k. [6]

El objetivo del proyecto ha sido el análisis de FSSs usando la Técnica de Resonancia Transversa para tres estructuras diferentes, usando circuitos equivalentes o directamente el valor de las susceptancias correspondientes a las superficies; para la última estructura estudiada, la susceptancia ha sido calculada a través de un software disponible, cuyo principal medio de operación está basado en el análisis modal que se explica en la sección 2.2, sin embargo, la complejidad de este análisis se ha visto reducida al utilizarse el análisis modal aplicado por el software, solamente sobre la superficie FSS y no sobre toda la estructura.

Con el fin de encontrar la solución de la ecuación que define la Técnica de Resonancia Transversa, fue necesario realizar una búsqueda de mínimo, tanto de mínimos dependientes de una variable (caso Surface-Wave) como de mínimos dependientes de dos variables, en el plano complejo (caso Leaky-Wave), sobre dicha función ya que en

7

determinados casos no era posible encontrar una solución analítica sin realizar aproximaciones. Este análisis se ha llevado a cabo con el fin de conseguir resultados precisos para los Diagramas de Dispersión y Radiación para las distintas estructuras en el plano H, de una forma rápida y sencilla. Además, como una posible ampliación de éste proyecto, en la sección de Conclusiones, la técnica que se ha implementado para el caso de una capa se puede extender a la aplicación para el caso de multicapas conociendo el coeficiente de reflexión total de la estructura. El análisis modal completo sobre toda la estructura para el caso de multicapas es algo complejo, así que el método que se ha presentado en este proyecto tiene una gran importancia en la caracterización de este tipo de antenas.

2 Técnicas de Análisis

Básicamente se pueden elegir tres maneras distintas de calcular las características de las FSSs. Estas tres formas están basadas en: métodos empíricos mediante la realización de medidas sobre las superficies, análisis modales y circuitos equivalentes.

2.1 Métodos empíricos

Este método consiste en la realización de varias medidas para diferentes formas y distribuciones de los elementos reactivas sobre la superficie. Una vez que estas medidas se han llevado a cabo, son comparadas con el objetivo de obtener resultados precisos. Este método está basado en la experiencia.

2.2 Análisis modales

La base de este método es el análisis de los campos electromagnéticos que aparecen en la estructura. Lo primero que hay que hacer en este análisis es relacionar los campos en la FSS con las corrientes inducidas en la pantalla debido a los campos incidentes. Una vez que dichas corrientes se han definido, a partir de éstas se pueden calcular otros parámetros de interés práctico como por ejemplo los coeficientes de reflexión y transmisión para los harmónicos dominantes.

2.3 Circuitos equivalentes

Una alternativa al análisis modal, antes de disponer de potentes ordenadores, fue el uso de modelos basados en circuitos equivalentes para encontrar las características electromagnéticas de la banda prohibida (*Electromagnetic Band Gap, EBG)*, de determinadas estructuras. Éstos son muy útiles a la hora de establecer de una manera rápida si una FSS puede dar una solución a un determinado diseño. Se corresponden con modelos empíricos, obtenidos mediante el ajuste experimental con medidas de los coeficientes de transmisión y reflexión en función de la frecuencia, y consecuentemente se requiere un modelo diferente para cada estructura. Los circuitos equivalentes definidos en el modelo se usan para calcular de una forma sencilla una aproximación de la frecuencia de la banda prohibida por medio de la aplicación de la Técnica de Resonancia Transversa.

Esta técnica está basada en el hecho de que en una guía de onda, a la frecuencia de corte, los campos forman ondas estacionarias en el plano transverso de la guía. Esta situación se puede modelar con un circuito equivalente para la estructura operando en resonancia (la *Figura 2* muestra un ejemplo de circuito equivalente). Una de las condiciones de una línea

en resonancia consiste en el hecho de que en cualquier punto de la línea con respecto al eje transversal a la dirección de propagación, la suma de las impedancias de entrada vistas a ambos lados de la línea en dicho eje debe ser cero. Esto es:

$$Z_{in}^{r}(z) + Z_{in}^{l}(z) = 0 \quad \text{para cualquier z (suponiendo que z es el eje transversal)} \quad (1)$$

Otra condición importante empleada en esta técnica se obtiene del hecho de que la constante de propagación en la dirección transversal al eje z (en nuestro ejemplo) , k_c, debe ser la misma en todas las regiones para que coincida la fase de los campos tangenciales en la superficie de contacto del dieléctrico.

De este modo, con $k_x=0$, se puede escribir la siguiente ecuación:

$$k_y = \sqrt{\varepsilon_r k_0^2 - k_{z_{gr}}^2} \, (dielectric) = \sqrt{k_0^2 - k_{z_0}^2} \, (air) \quad (2)$$
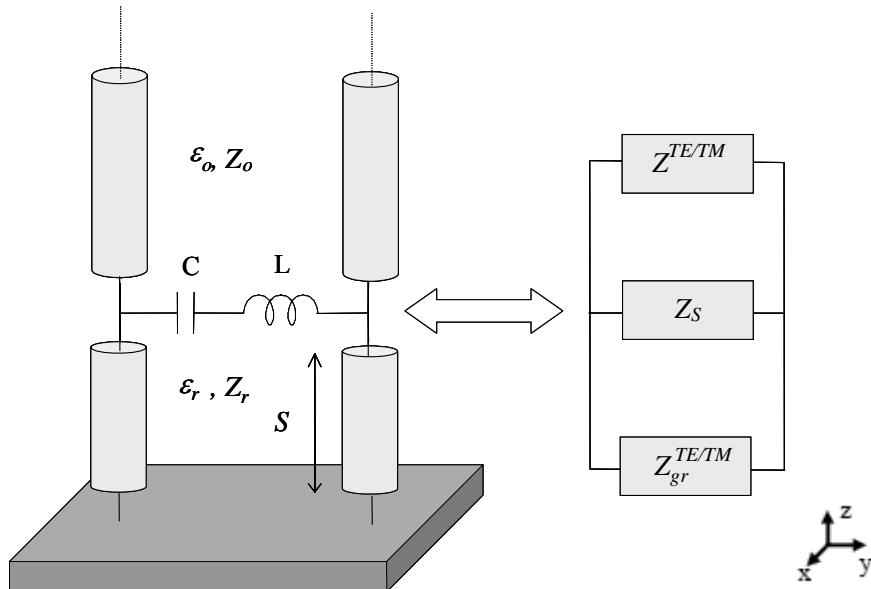
Figura 2. Ejemplo de modelo equivalente con dieléctrico sobre un plano de masa.[5]

Las ecuaciones (1) y (2) se usan finalmente para obtener la constante de propagación que nos permite construir el Diagrama de Dispersión de la estructura (k_y vs. f(GHz)). Se tiene que tener en cuenta que la Técnica de Resonancia Transversa sólo es válida a la frecuencia de corte de la guía. Si son necesarios la obtención de los campos electromagnéticos o atenuaciones debido a las pérdidas del conductor, se requiere hacer un análisis completo de la teoría de campos.

3 Aplicaciones

3.1 Surface-Wave antenas

En esta sección del informe, se estudiará una estructura que opera como una antena Surface-Wave. Las antenas Surface-Wave radian en dirección end-fire (ver *Figura 3*). La estructura de guía básica para este tipo de antenas es una guía de onda abierta cuyo modo dominante (onda de superficie o Surface-Wave) está exclusivamente ligado a la superficie, así que radiará sólo ante discontinuidades como la que se encuentra al final de una guía. Este tipo de antenas no radia a lo largo de la guía debido a que la onda de superficie es una onda lenta, es decir $\beta > k_0$, siendo k_0 el número de onda de espacio libre en el aire. El número de onda, o constante de propagación, es en este caso real y formado sólo por una constante de fase, $k_p = \beta$.
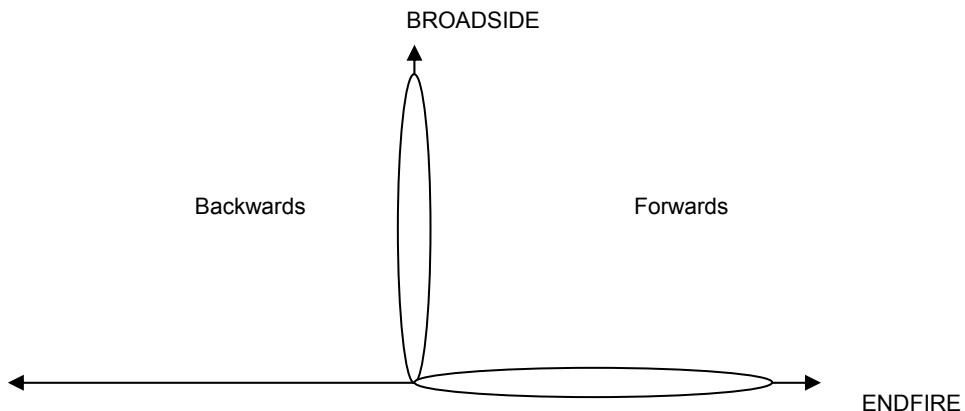
Figura 3. Direcciones de radiación de una antena. Endfire se corresponde con la dirección de propagación en el plano de la antena y Broadside, con la dirección perpendicular al plano de la misma.

3.1.1 Estructura 1

La primera estructura que se va a estudiar es la representada en la *Figura 4 a)*. Esta estructura está compuesta por tripolos y es usada en [3] como una estructura electromagnética miniaturizada de banda prohibida (MEBG) para aplicaciones móviles. Como las MEBGs se componen de elementos resonantes, la dimensión de cada elemento es aproximadamente la mitad de la longitud de onda, así que para dispositivos operando a altas frecuencias, se requiere una miniaturización para su integración en los nuevos terminales móviles.
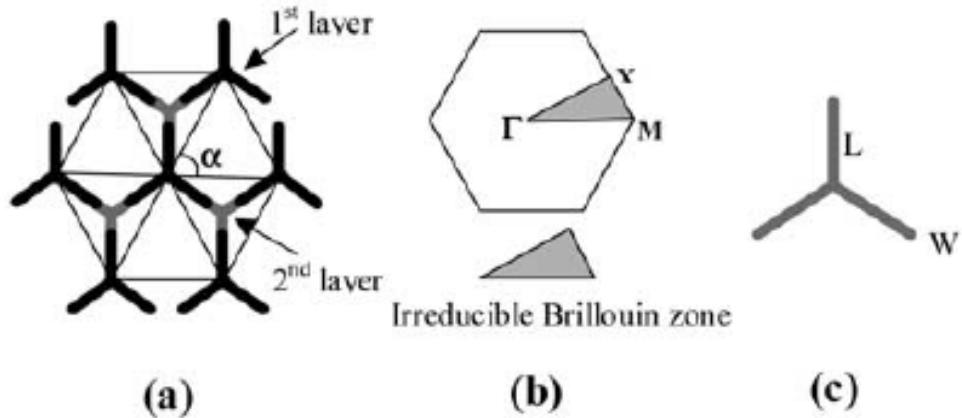
Figura 4. a) Tripoles structure, **b)** estructura recíproca y su irreducible zona Brillouin, y **c)** dimensiones de los tripolos L=5mm, W=0.5 mm, periodicidad D=12mm, ε_r=2.2, grosor s=1.13mm, y α=60°. [3]

El objetivo para esta estructura es conseguir el Diagrama de Dispersión a partir de su circuito equivalente, aplicando la Técnica de Resonancia Transversa.

Como se muestra en la *Figura 5*, el circuito equivalente para una celda unitaria de la superficie está formado por dos líneas de transmisión correspondientes con el aire que se encuentra en la parte superior e inferior de la FSS, una capacitancia y una inductancia. La superficie se supone suspendida en aire así que las líneas de transmisión se consideran infinitas, con $\varepsilon_r = 1$.
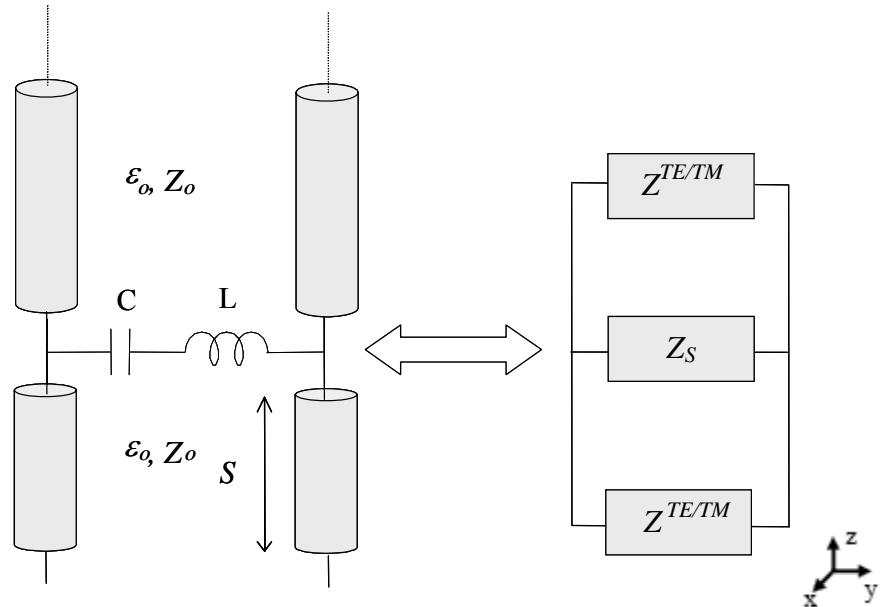
Figura 5. Circuito equivalente de una celda unitaria de la estructura de la *Figura 4*.

Cuando se aplica la Técnica de Resonancia Transversa estudiada en la sección 2.3., se derivan las siguientes ecuaciones a partir de (1):

$$Y_s + 2 \cdot Y_0 = 0 \qquad (3)$$

12

Donde:

$Y = \dfrac{1}{Z}$ (en general).

$Z_s = jwL + \dfrac{1}{jwC}$, y

$Z_0^{TE} = \dfrac{k_0 \cdot \eta_0}{k_z} = \dfrac{w \cdot \mu_0}{k_z}$, (sólo se va a estudiar el caso TE).

Con el fin de obtener una solución analítica para la constante de propagación en la dirección del eje y (suponiendo que no hay propagación en el eje x), se aplican (1) y (2).

La solución analítica final es la siguiente:

$$k_{TE} = \frac{w}{c}\sqrt{1 + 0.25\left[\frac{wC\eta_0}{1 - \left(\frac{w}{w_0}\right)^2}\right]^2} \qquad (4)$$

Donde η_0 representa la impedancia intrínseca del espacio libre y $w_0 = 1/\sqrt{LC}$, es la frecuencia de resonancia del circuito LC en serie que representa al array (ver desarrollo en el Apéndice II).

Esta solución analítica se implementó en Matlab para obtener el Diagrama de Dispersión para L=2nH, C=0.41pF (caso de estructura gruesa, thick, W=5mm) y C=13.28pF (caso de estructura miniaturizada, thin, W=0.5mm) del primer TE modo para la dirección ΓM. El Diagrama de Dispersión para ambos casos representado en Matlab es el que muestra la *Figura 6*.
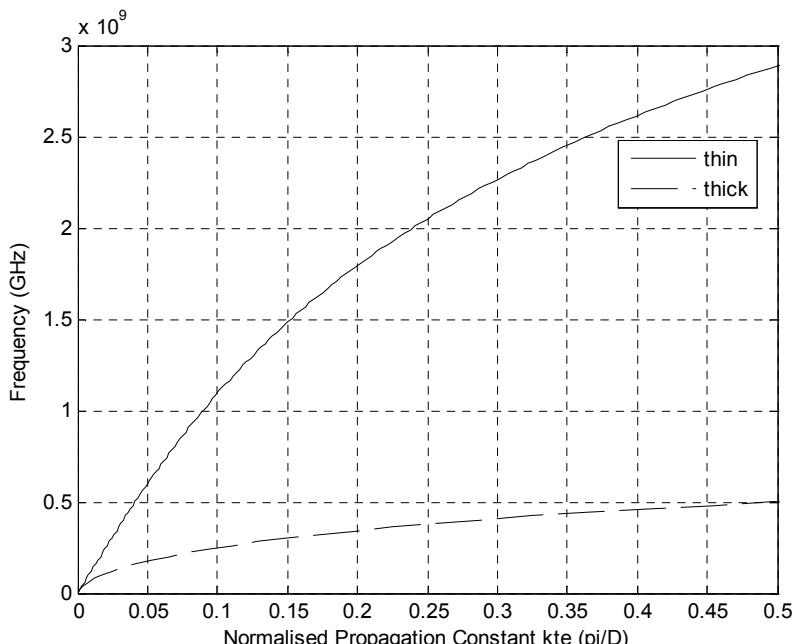
Figura 6. Diagrama de Dispersión para tripolos finos y gruesos. Solución analítica.

13

Para este simple caso en el que se supone la estructura suspendida en aire, sin otro tipo de dieléctrico o plano de masa, fue sencillo conseguir una solución analítica para la constante de propagación. Aunque en el caso en el que hubiera plano de masa, no se podría obtener una solución analítica debido al elemento cotangente que aparecerá en el caso de la *estructura 2*. Por esta razón, en este proyecto se ha implementado un método eficiente y rápido para conseguir una solución precisa para la constante de propagación. Este método consiste en calcular el valor de la constante de propagación que hace mínima la función (1). Primero se toma un rango de valores para la constante de propagación, teniendo en cuenta que esta estructura se está estudiando como una antena Surface-Wave, así que la constante de propagación debe cumplir que $k_y = \beta > k_0$. A continuación, todos los posibles valores que toma k_y en el rango original tomado, se aplica a la ecuación (3) que define la Técnica de Resonancia Transversa para una determinada frecuencia. Finalmente, el valor de k_y que hace el valor absoluto de la función mínimo (mediante el uso de la función *min* de Matlab), es la solución para dicha frecuencia. Las *Figuras 7 y 8* muestran un ejemplo visual de cómo se ha calculado el mínimo del valor absoluto de la función (3) para una frecuencia de 0.5GHz.
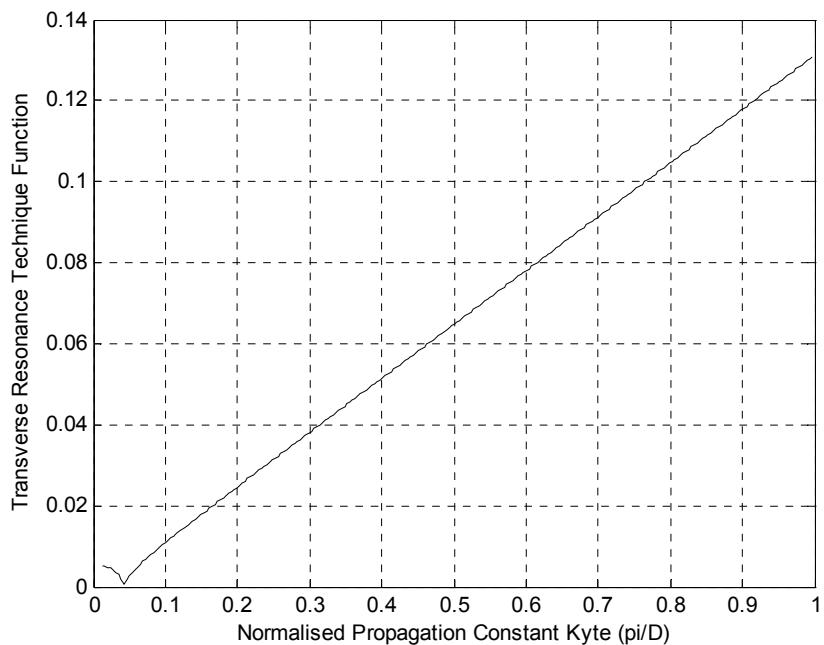
Figura 7. Caso tripolos finos (thin). Representación de los valores que toma la función (3) en **valor absoluto** que define la Técnica de Resonancia Transversa para la frecuencia f=0.5GHz, en función de $k_y=\beta$ para todo el rango inicial.
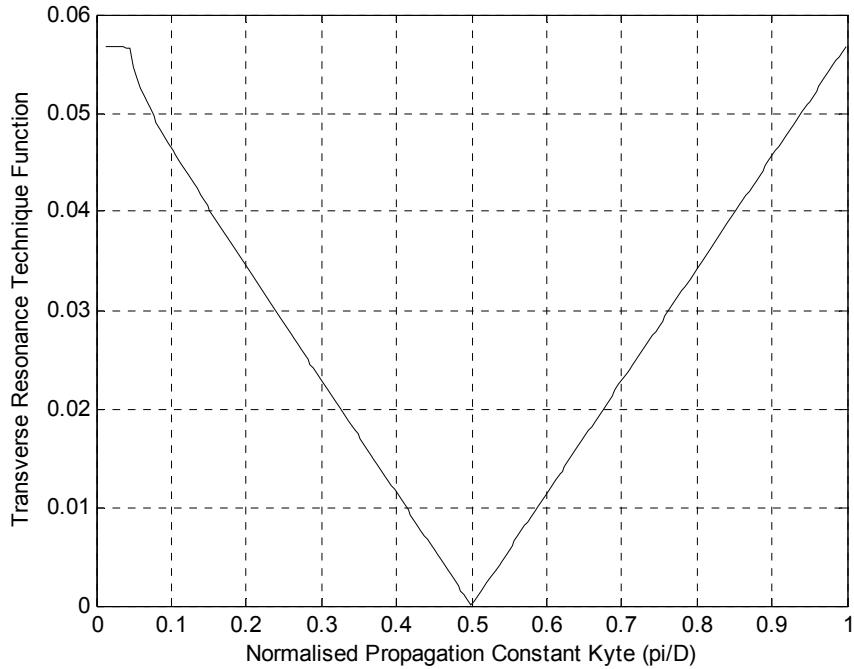
Figura 8. Caso tripolos gruesos (thick). Representación de los valores que toma la función (3) **en valor absoluto** que define la Técnica de Resonancia Transversa para la frecuencia f=0.5GHz, en función de $k_y=\beta$ para todo el rango inicial.

Además, cuando k_z se calcula como $k_z = \sqrt{k^2 - k_c^2}$, se obtiene un valor imaginario y positivo para k_z, lo que significa que la constante de atenuación en el eje z sería negativa. Recordad que la expresión de la constante de propagación es $k_z = -j\alpha$. Debido a que no tiene sentido para ondas de superficie tener una constante de atenuación negativa en el eje z, es decir, tener un incremento de energía según se avanza en dicho eje, con el fin de obtener la correcta solución fue necesario tomar como válida la solución negativa de la raíz cuadrada. En las siguientes estructuras que se estudiarán a lo largo de este proyecto, debido a que actúan como Leaky-Wave antenas, se debe tomar la solución positiva de la raíz cuadrada en el caso de propagación en dirección forward, debido a que la contribución del resto de celdas provocan un aumento de energía en la dirección z, es decir, producen una constante de atenuación negativa a lo largo de éste eje. Ver [19] para entender con más detalle este fenómeno.

Esta sencilla estructura se ha estudiado con el fin de comparar la solución obtenida con este nuevo método y la solución analítica. La *Figura 9* muestra la solución obtenida con el método de búsqueda de mínimo, y como se ha podido observar, se han conseguido soluciones similares; por lo tanto, se ha verificado el método implementado en este proyecto para esta estructura.

15
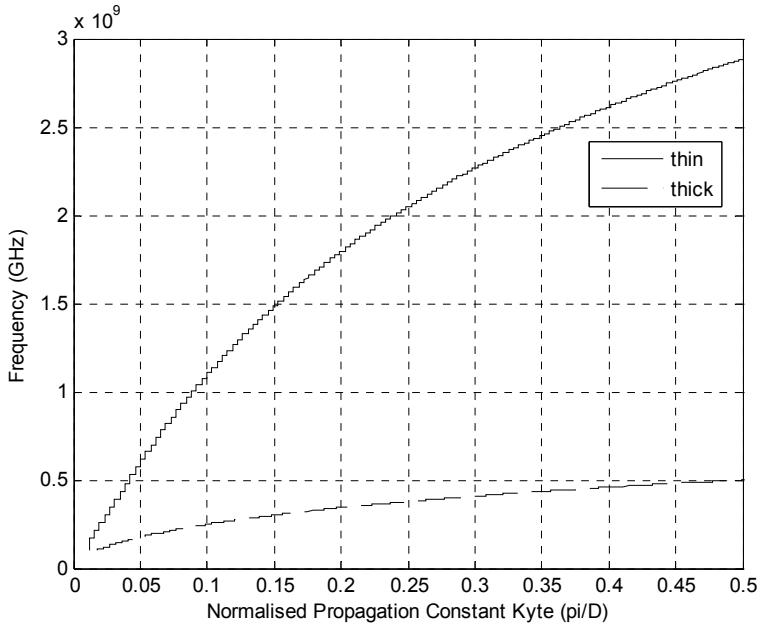
Figura 9. Diagrama de Dispersión para tripolos finos y gruesos. Solución aplicando el nuevo método.

3.2   Leaky-Wave antenas

En esta sección se van a estudiar dos estructuras diferentes que operan como antenas Leaky-Wave (LW). Este tipo de antenas son atractivas debido a la simplicidad de su estructura, fácil fabricación e integración de otros componentes de tecnología planar. Las antenas Leaky-Wave periódicas están a menudo basadas en guías de onda de superficie. La guía de onda básica puede ser una estructura abierta cuyo modo dominante es una onda de superficie, que es una onda lenta, y la radiación se produce colocando arrays periódicos de discontinuidades en la guía de manera que el primer armónico se convierte en rápido, es decir $\beta < k_0$, consecuentemente la antena radia.

Las antenas Leaky-Wave no radian bien en la dirección end-fire y, de hecho, son diseñadas para radiar en cualquier otra dirección o barrer un rango de ángulos. La intención de estas antenas es producir una pequeña fuga por unidad de longitud; de este modo, cada elemento que produce una discontinuidad en el array periódico de elementos, produce una pequeña carga sobre el modo básico de la guía de onda. Como resultado, el proceso de diseño ve las antenas Leaky-Waves como una estructura equivalente homogénea con una constante de propagación compleja, $k_p = \beta_p - j\alpha_p$. Por lo tanto, el número de onda está compuesto por una constante de atenuación o fuga, α, y una constante de fase, β. La variable α es grande o pequeña dependiendo de si la atenuación por unidad de longitud es mayor o menor. Otra característica a tener en cuenta es que a causa de que la constante de fase β cambia con la frecuencia, la antena puede barrer distintos ángulos mediante la variación de ésta.

16

3.2.1 Estructura 2

La siguiente estructura que se va a estudiar se corresponde con la presentada en [15]. El modelo equivalente de esta estructura se muestra en la *Figura 10*. Por lo tanto, a partir de este modelo, se puede aplicar fácilmente la Técnica de Resonancia Transversa.

Para esta estructura los parámetros son: S=5mm, $\varepsilon_r = 2.2$, $\mu_r = 1$, y $\overline{B}_s = 20$, siendo ésta última la susceptancia (parte imaginaria de la admitancia) que representa la FSS, donde la barra significa normalización mediante multiplicación por la impedancia característica en el espacio libre η_0.
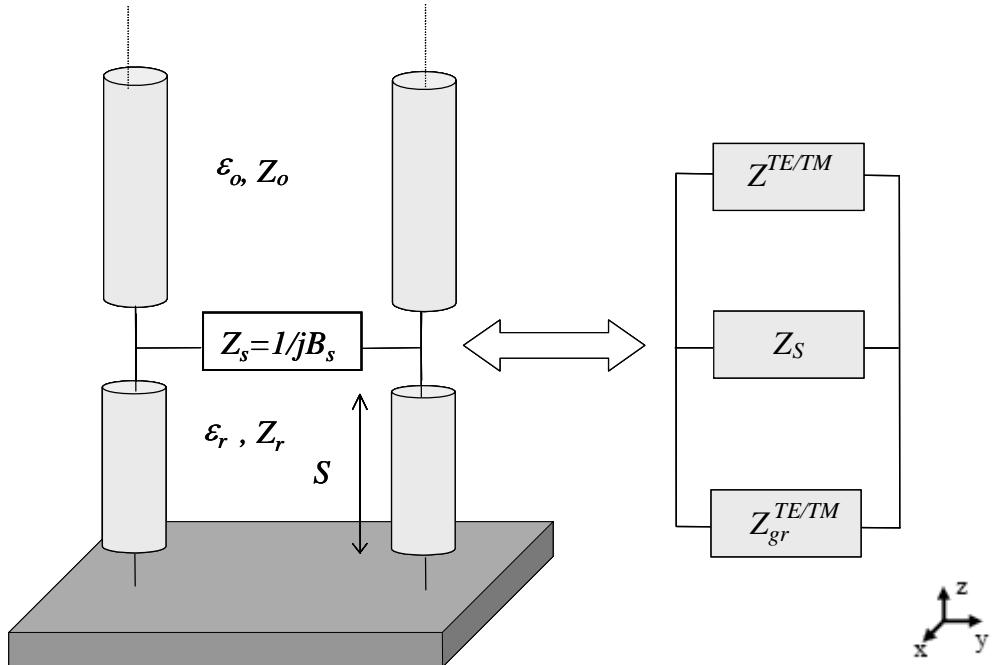
Figura 10. Modelo equivalente sobre dieléctrico conectado a un plano de masa.

La función que define la Técnica de Resonancia Transversa para la *estructura 2*, es la siguiente:

$$Y_S + Y_0^{TE} + Y_{gr}^{TE} = 0 , \qquad (5)$$

Donde:

$$Y_S = j\overline{B}_s , \quad Y_0^{TE} = \frac{k_{z_0}}{k_0\eta_0} = \frac{k_{z_0}}{w\mu_0} \text{ y } Y_{gr}^{TE} = -j\frac{k_{z_{gr}}}{k_0\eta_0\mu_r}\cot\left(k_{z_{gr}}S\right).$$

Con el fin de calcular k_y a partir de k_z en el código realizado en Matlab, k_z es reemplazada usando (2) en las correspondientes ecuaciones de las admitancias.

17

La diferencia con la primera estructura es que ahora, se estudia el correspondiente modo Leaky-Wave TE que se propaga en esta estructura, así que a la hora de buscar el mínimo de la función que define la Técnica de Resonancia Transversa, se tienen que tener en cuenta dos parámetros , α y β. Con este objetivo, se elige un rango de valores para α y β y se sustituyen en (5) todas las posibles combinaciones de estos dos parámetros. Finalmente la combinación que hace mínima la función para cada frecuencia, es la solución buscada para esa misma frecuencia. Como ejemplo visual de esta búsqueda de mínimo en el plano complejo, la *Figura 11* representa en tres dimensiones el valor absoluto de la función (5), en función de α y β para una frecuencia de 20.8GHz.
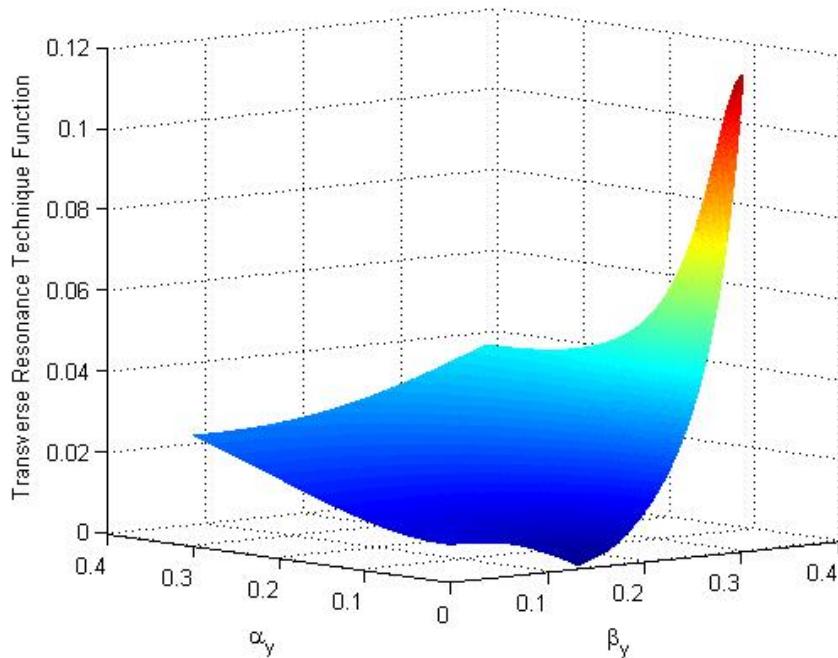
Figura 11. Representación en tres dimensiones de los valores que toma la función (5) **en valor absoluto**, que define la Técnica de Resonancia Transversa para la frecuencia f=20.8GHz, en función de β y α.

Aplicando el método de búsqueda del mínimo para (5) en todo el rango de frecuencias dado, el resultado obtenido para el Diagrama de Dispersión es el mostrado en la *Figura 12*.

Como se puede observar, usando el método implementado en este proyecto se han obtenido resultados similares a los obtenidos en [15], lo que verifica una vez más esta técnica. La condición α =β representa la condición de separación del lóbulo principal en el Diagrama de Radiación, entre el caso en el que éste apunta exactamente a Broadside (cuando β< α) y cuando éste se ha dividido y forma dos picos (cuando β> α). Nota: $\sin(\theta_0) \approx \dfrac{\beta}{k_0}$, donde es el ángulo de máxima radiación, medido a partir de la dirección Broadside (ver *Figura 13)*.
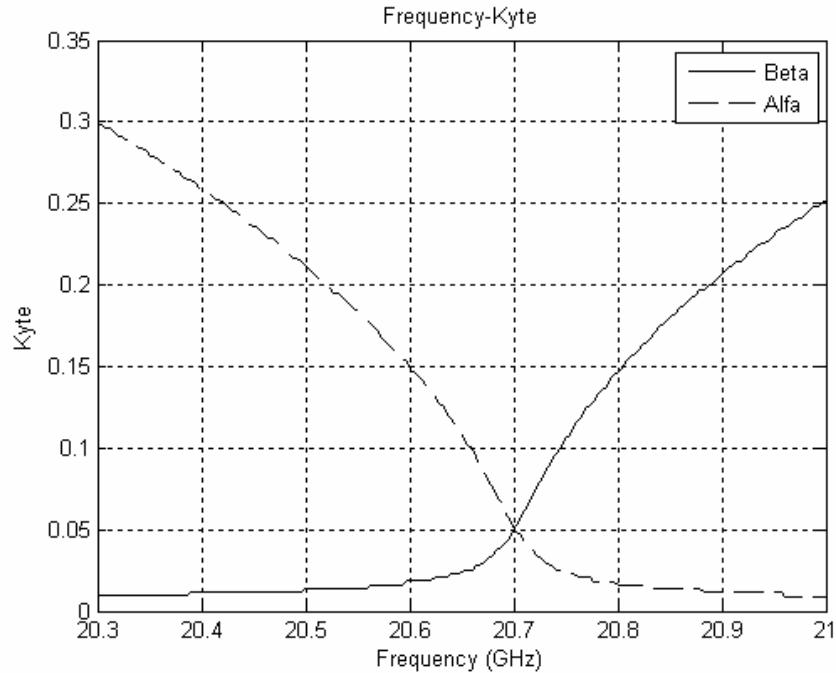
Figura 12. Constantes de fase ($\hat{\beta}$) y atenuación ($\hat{\alpha}$) normalizadas en función de la frecuencia f para el correspondiente modo TE Leaky-Wave de una LW antena. Parámetros: S=5mm, $\varepsilon_r = 2.2$, $\mu_r = 1$, y $\overline{B}_s = 20$.
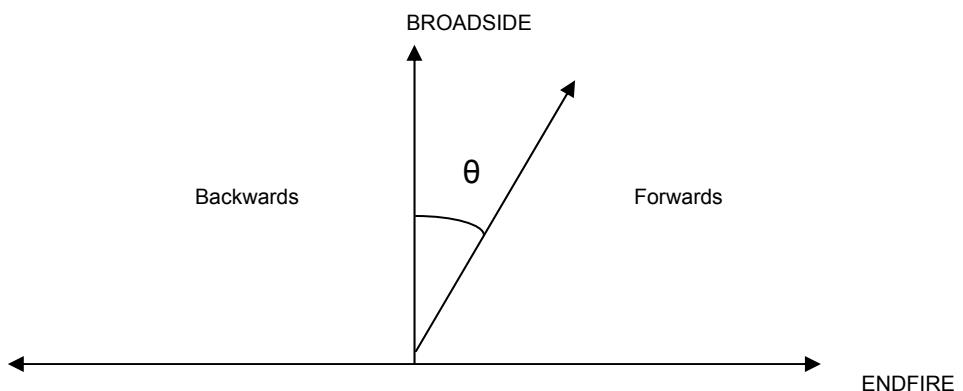

Figura 13. Direcciones de radiación de una antena. Endfire se corresponde con la dirección de propagación en el plano de la antena y Broadside, con la dirección perpendicular al plano de la misma. θ representa el ángulo de escaneo de una antena.

3.2.2 Estructura 3

3.2.2.1 Análisis.

La estructura representada en la *Figura 14* cubre es estudio más importante de este proyecto. Consiste en una superficie de dipolos dispuestos periódicamente sobre ésta, suspendida en aire, a una distancia S del plano de masa. En las estructuras anteriores, el método utilizado para obtener el Diagrama de Dispersión de la antena fue mediante la aplicación de circuitos equivalentes o conocido el valor de la admitancia correspondiente a una FSS específica. En esta estructura, se hizo uso de un programa disponible, implementado en Fortran (Apéndice I), con el fin de calcular la admitancia que representa la superficie, FSS (*Figura 15*).

a)

b)
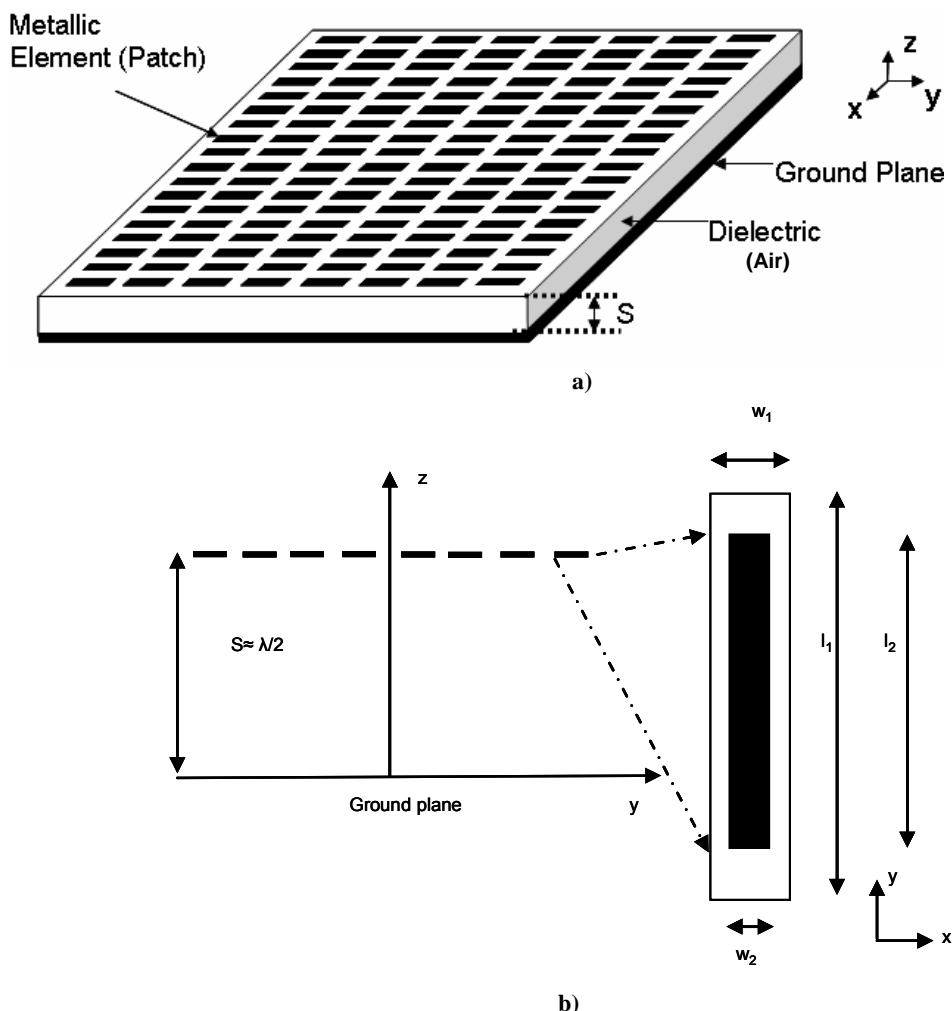
Figura 14. Esquema general de la antena Leaky-Wave, **a)**, y detalle de una celda unitaria, **b)**. Datos: w_1=1.5 mm , w_2=0.5 mm, l_1=11 mm, l_2=10 mm and S=h=11.1 mm. El espesor del dieléctrico sobre el que se sostiene la FSS es 1.13 mm, y su permitividad relativa $\varepsilon_r = 2.2$.

20

El programa en Fortran da como resultado, entre otros, el coeficiente de reflexión de la FSS para cada frecuencia estudiada, usándose posteriormente para calcular la admitancia de la superficie. Debido a que estos resultados se calculan en el programa suponiendo que la FSS está suspendida en el aire, lo que equivale a una línea de transmisión infinita, la admitancia de la superficie se puede calcular fácilmente a partir de la siguiente ecuación:

$$\Gamma = \frac{Z_{in} - Z_0}{Z_{in} + Z_0} \qquad (6)$$

Donde Γ es el coeficiente de reflexión visto desde la flecha indicada en la *Figura 15*, Z_{in} la impedancia de entrada vista desde el mismo punto, y Z_0 la impedancia característica de las líneas de transmisión.

Ya que la línea de transmisión es infinita, la *Figura 15* se puede modificar como se muestra en la *Figura 16*, de manera que la ecuación (6) se reescribe de la siguiente manera:

$$\Gamma = \frac{Z_S // Z_0 - Z_0}{Z_S // Z_0 + Z_0} \qquad (7)$$

Donde $Z_S // Z_0$ se refiere al resultado del paralelo de las impedancias Z_S y Z_0.
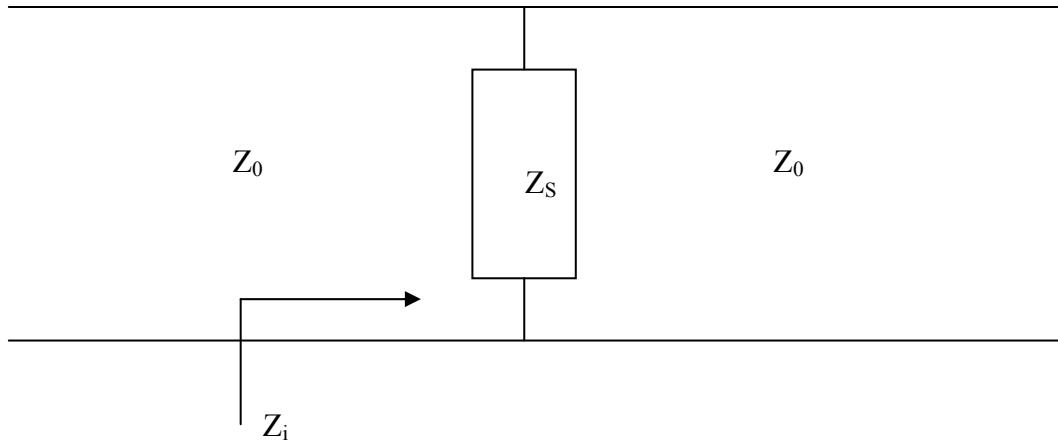
Figura 15. Modelo equivalente para el caso ideal donde las líneas de transmisión son infinitas (FSS suspendida en aire) correspondiente con el caso representado en el programa en Fortran. Z_s es la impedancia correspondiente a la FSS.

Resolviendo (7) y sabiendo que la admitancia es la inversa de la impedancia, el resultado para Y_S es el siguiente:

$$Y_S = -\frac{2\Gamma}{Z_0(1+\Gamma)} \qquad (8)$$

21
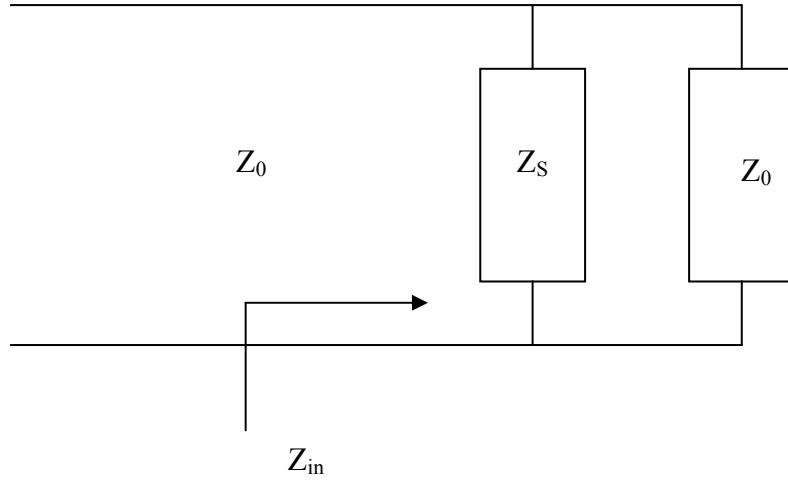
Figura 16. Modelo equivalente derivado de la *Figura 12,* debido a que la línea de transmisión es infinita.

Una vez que se ha calculado la admitancia de la FSS, se puede aplicar la Técnica de Resonancia Transversa a partir del modelo equivalente de la celda unitaria de la estructura, mostrado en la *Figura 17*. La expresión en este caso se expresa como se muestra a continuación:

$$Y_S + Y_0^{TE} + Y_{gr}^{TE} = 0 \qquad (9)$$

Donde:

Y_S es el resultado de (8), $Y_0^{TE} = \dfrac{k_{z_0}}{k_0\eta_0} = \dfrac{k_{z_0}}{w\mu_0}$ y $Y_{gr}^{TE} = -j\dfrac{k_{z_0}}{k_0\eta_0}\cot\left(k_{z_0}S\right)$.

Con el fin de calcular k_y a partir de k_z en el código implementado en Matlab, directamente, k_z se sustituye usando (2) en las correspondientes ecuaciones para las admitancias.
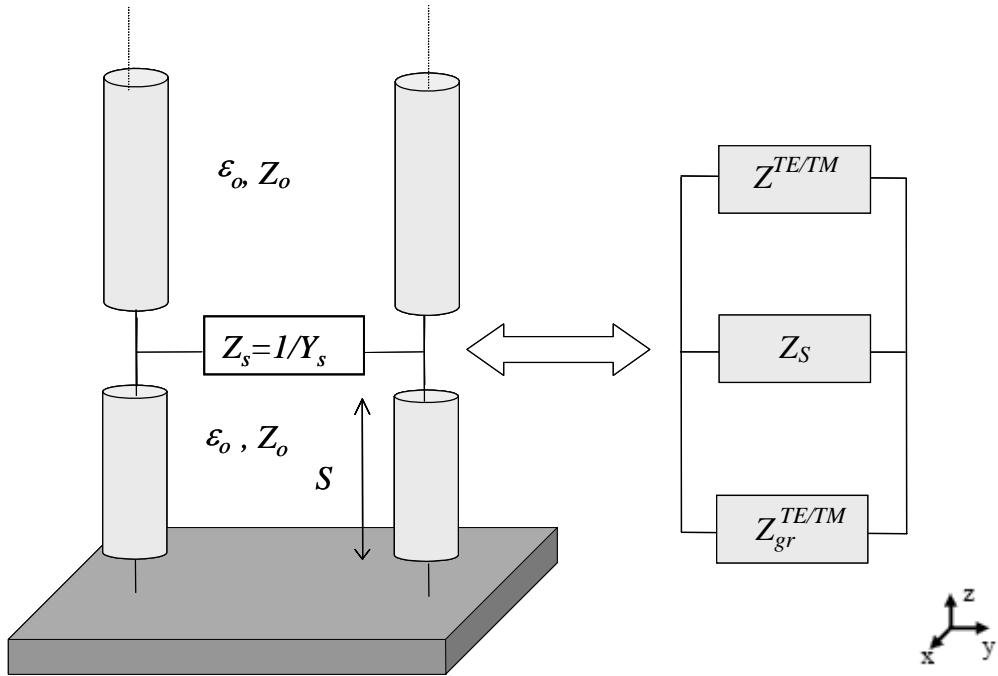
Figura 17. Modelo equivalente de una celda unitaria de la estructura mostrada en la *Figura 11*.

Una vez que se han calculado todos los datos para poder obtener el Diagrama de Dispersión, se ha aplicado el método de búsqueda de mínimo a la función (9), obteniéndose los siguientes resultados mostrados en las *Figuras 18 y 19* para las constantes de fase y atenuación en función de la frecuencia, respectivamente:
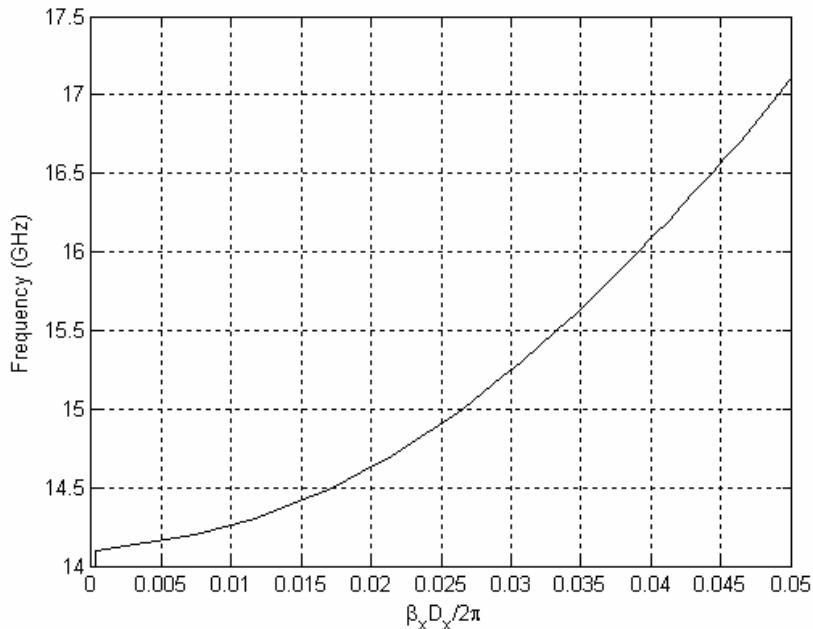

Figura 18. Constante de fase ($\hat{\beta}$) normalizada, en función de la frecuencia f para el correspondiente modo TE Leaky-Wave de una antena LW. Datos: w_1=1.5 mm , w_2=0.5 mm, l_1=11 mm, l_2=10 mm y S=h=11.1 mm. El espesor del dieléctrico sobre el que se sostiene la FSS es 1.13 mm, y su permitividad relativa $\varepsilon_r = 2.2$.

Por debajo de la frecuencia de corte, hay una banda de paro y por lo tanto no hay propagación para este modo. Sobre la frecuencia de corte, se encuentra una banda de paso correspondiente con el modo que se muestra en la *Figura 18,* donde la onda se propaga.
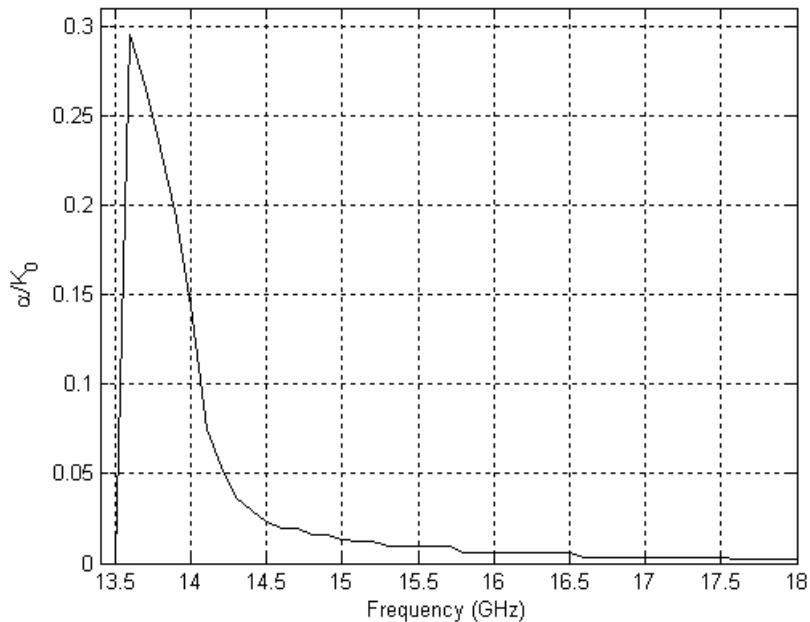

Figura 19. Constante de atenuación ($\hat{\alpha}$) normalizada, en función de la frecuencia f para el correspondiente modo TE Leaky-Wave de una antena LW. Datos: w_1=1.5 mm , w_2=0.5 mm, l_1=11 mm, l_2=10 mm y S=h=11.1 mm. El espesor del dieléctrico sobre el que se sostiene la FSS es 1.13 mm, y su permitividad relativa $\varepsilon_r = 2.2$.

Como se puede observar, por debajo de la frecuencia de corte el valor de α es muy elevado debido a que a esas frecuencias existe una banda de paro. Una vez alcanzada la frecuencia de corte, la constante de atenuación decrece a valores normales.

Los resultados obtenidos fueron difíciles de encontrar debido a que aplicando el método de búsqueda de mínimos aplicado anteriormente, el valor mínimo que el programa encontraba para determinadas frecuencias era el mínimo que se encontraba en la asíntota correspondiente con el máximo valor de beta en el rango elegido inicialmente, como se puede observar en la *Figura 20.* Con el objetivo de resolver este problema, una vez estudiada la función mostrada en dicha figura, se necesitó añadir una parte de código en el que se realizaba una comparación de signos de los gradientes de la función para un valor fijo de α, en función solamente de β. Una vez encontrado este punto, la matriz total que contenía los valores de la función, se reducía a una matriz de dimensión en β igual al punto obtenido como primer mínimo más un margen de error en el caso de que variara la situación del mínimo total en función de la variable α. De esta manera, nos aseguramos que el mínimo que encontraba se correspondía con el primero, no con el encontrado en la asíntota (ver informe en inglés para más detalle).

24
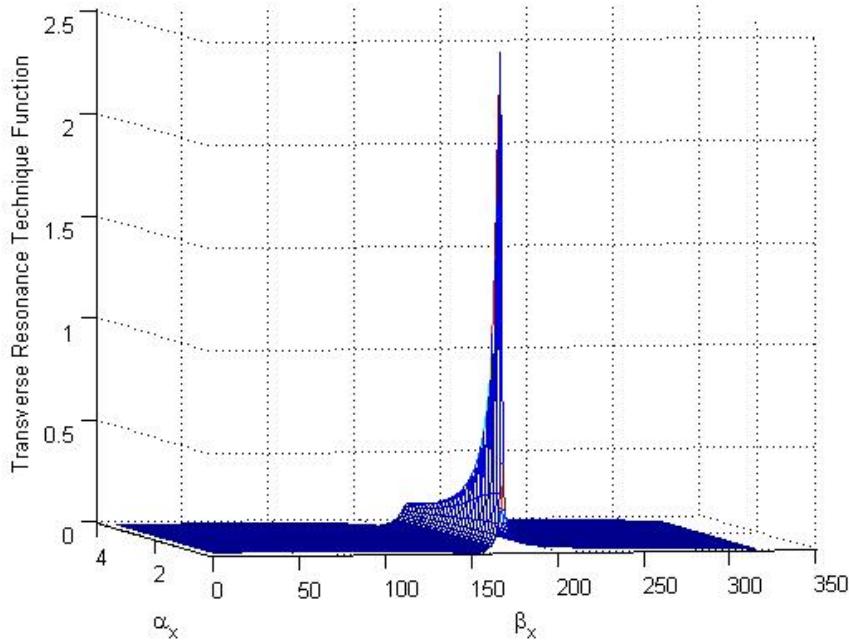
Figura 20. Representación en tres dimensiones de los valores que toma la función (9) **en valor absoluto**, que define la Técnica de Resonancia Transversa para la frecuencia f=15.8GHz, en función de β y α.

3.2.2.2 Comportamiento de la antena

Una de las características más importantes para el estudio del comportamiento de una antena es su Diagrama de Radiación. El Diagrama de Radiación de una antena es la representación de la magnitud del campo en la zona lejana contra posición en la antena, a una distancia fija de ésta. El diagrama puede presentar distintos lóbulos, con diferentes máximos en diferentes direcciones. El lóbulo que presenta máximo valor se llama lóbulo principal mientras que los adyacentes de inferior nivel son llamados lóbulos secundarios.

Con el fin de obtener el Diagrama de Radiación para la estructura mostrada en la *Figura 14*, se ha usado el Principio de Aproximación por el Factor de Array expuesto en [12].

Este principio establece que una antena Leaky-Wave se puede considerar como un array de antenas en fase con espaciado *p* entre elementos en el límite en el que $p \to 0$, como se ilustra en la *Figura 21*. Mientras que el array en fase, *Figura 21 a)*, es alimentado discretamente a cada elemento n^{th} con una función de fase $\xi_n(\theta_0)$ (Siendo θ_0 el ángulo de radiación) y una función de magnitud constante $I_n = I_0 (\forall n)$, la antena Leaky-Wave en la *Figura 21 b)* se alimenta de forma continua solamente al extremo de la estructura con una función de fase $\xi(\theta_0)$ y una función de magnitud exponencial $I(x) = I_0 \exp(-\alpha x)$, donde α es el factor de fuga o atenuación.
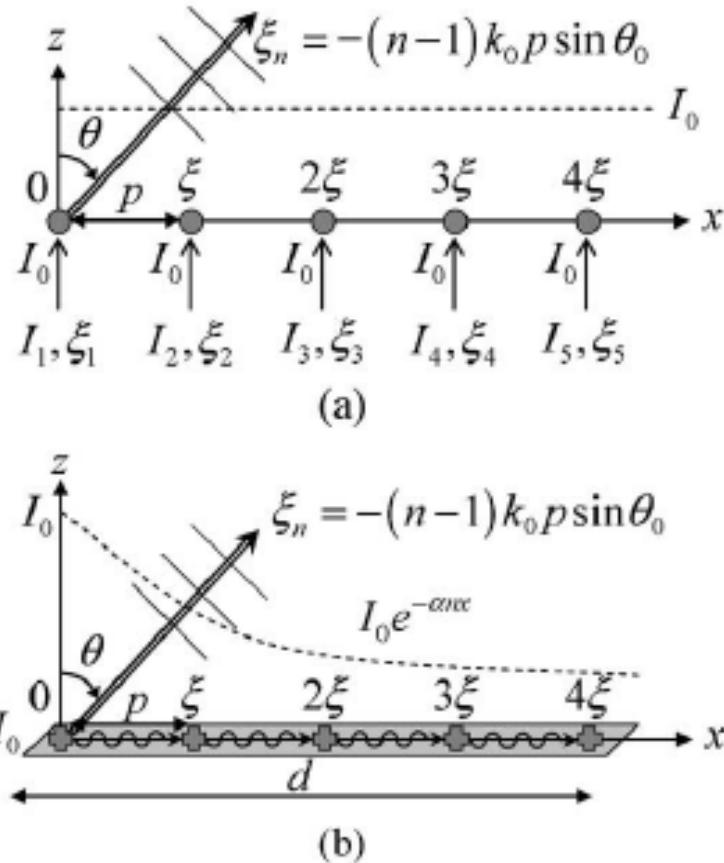
Figura 21. Principio de Aproximación por el Factor de Array. (a) Configuración discreta de una array en fase convencional con separación entre elementos p. (b) Configuración continua de una estructura periódica para una antena Leaky-Wave con periodo p. [12]

De esta manera, en el caso de estructuras LW para metamateriales se cumple la condición $p \rightarrow 0$, o más significativo $p / \lambda_g \rightarrow 0$, debido a la definición de un medio efectivo. Por lo tanto las funciones de fase y magnitud se pueden discretizar como:

$$\xi_n = -(n-1)k_0 p \sin \theta_0 \quad \text{y} \quad I_n = I_0 e^{-\alpha(n-1)p} \qquad (10)$$

Donde p se corresponde con la periodicidad en la estructura y k_0 es el número de onda en el espacio libre. Ya que $p / \lambda_g \rightarrow 0$, cada contribución por cada incremento en la periodicidad será equivalente a un elemento isotrópico radiante y el diagrama de radiación total $R(\theta)$ de la antena LW se puede aproximar por la función del factor de array:

$$R(\theta) = AF(\theta) = \sum_{n=1}^{N} I_n e^{j(n-1)k_0 p \sin \theta + j\xi_n} \qquad (11)$$

Donde N representa el número de celdas unitarias que constituyen la estructura con las funciones ξ_n y I_n dadas por (10). En general, para antenas LW el ángulo de radiación en (19) es dado por:

$$\theta_0 = \sin^{-1}\left[\frac{\beta(w)}{k_0}\right] \qquad (12)$$

Donde $\beta(w)$ es la constante de propagación de la dirección de propagación en la estructura.

El Diagrama de Radiación para la *estructura 3* se ha calculado para una determinada frecuencia, usando el método explicado anteriormente. Además, para una antena LW bidireccional, como la que se muestra en la *Figura 22*, la contribución de ambos polos k_p y $-k_p$ (being $k_p = \alpha_p + i\beta_p$) se tienen que tener en cuenta en la ecuación.
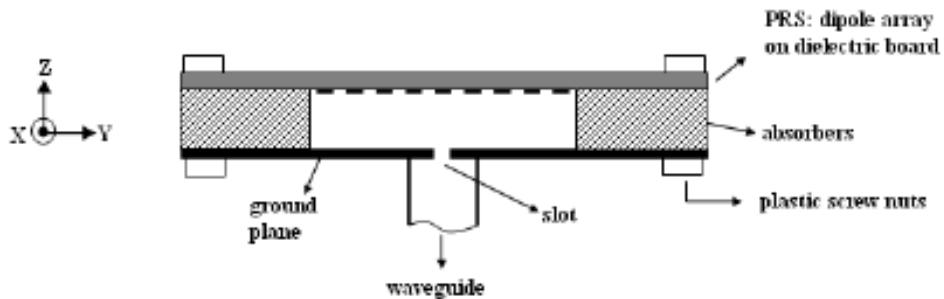
Figura 22. Esquema de una antena bidireccional. La delgada capa de dieléctrico se coloca para sostener la PRS (Partially Reflective Surface) o FSS y mejorar la precisión en las medidas. [16]

Con el fin de calcular el Diagrama de Radiación para una antena bidireccional, que sería nuestro caso, el resultado es la superposición de las contribuciones de (11) para valores positivos y negativos de k_p (constante de propagación en la dirección de propagación sobre la superficie) pero calculadas para la mitad de la longitud total de la antena, L. El valor absoluto de la solución en (11) para valores positivos y negativos de k_p se multiplican y el producto se divide por el máximo valor de este mismo producto para ser normalizado, es decir, se normaliza por el valor de intensidad de máxima radiación. Finalmente, para conseguir el Diagrama de Radiación final, los resultados para diferentes frecuencias se representan en escala logarítmica. De esta manera, se aplicó la siguiente ecuación:

$$20\log\left(\frac{\left.|F(\theta,\phi)|\right|_{k_{positive}} \cdot \left.|F(\theta,\phi)|\right|_{k_{negative}}}{\max\left(\left.|F(\theta,\phi)|\right|_{k_{positive}} \cdot \left.|F(\theta,\phi)|\right|_{k_{negative}}\right)}\right) \qquad (13)$$

La representación correspondiente con el Diagrama de Radiación calculado mediante el método que ha sido expuesto, para 15GHz, se muestra en la *Figura 23* y es comparado con medidas reales usadas en [16] para la misma estructura.
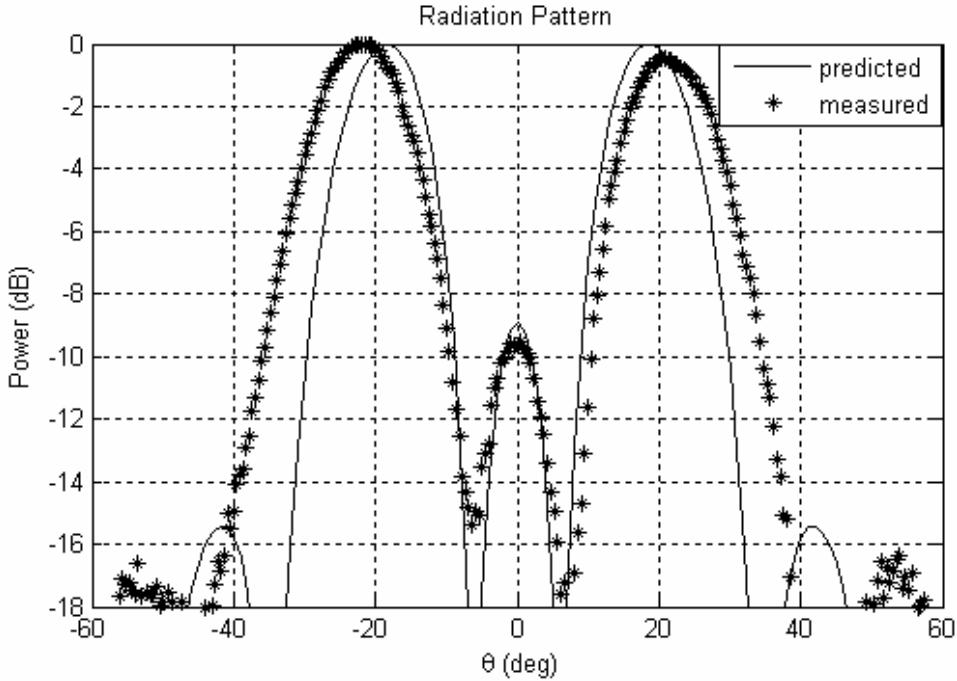

Figura 23. Comparación del Diagrama de Radiación calculado con el método realizado en este proyecto y con los resultados medidos en [16], para una frecuencia de 15GHz.

Como se puede observar, los resultados obtenidos con el método implementado en este proyecto y los obtenidos a través de medidas reales son muy próximos, una vez más nuestro método ha sido verificado. Sin embargo, se pueden observar ciertas discrepancias debido a las limitaciones que poseen los experimentos reales. Esto podría ser debido a los efectos de difracción en los bordes del metal y el material absorbente, o errores de posicionamiento o alineación, lo que puede causar pérdidas de simetrías en el patrón.

La comparación con medidas reales ha sido realizada gracias a anteriores experimentos realizados en el departamento de Ingeniería Electrónica y Eléctrica de la Universidad de Loughborough (Inglaterra), en el grupo de Comunicaciones Inalámbricas, donde este proyecto se ha llevado a cabo. La antena que se diseño en trabajos anteriores en este departamento se muestra en las imágenes de las *Figuras 24 a) y b)*, y las medidas se realizaron en la cámara anecoica mostrada en la *Figura 24 c)*. Básicamente una cámara anecoica es una sala especialmente diseñada para absorber las ondas que inciden sobre las paredes, el suelo y el techo de la misma cámara, anulando los efectos de reflexión de la onda.

a)

b)

c)
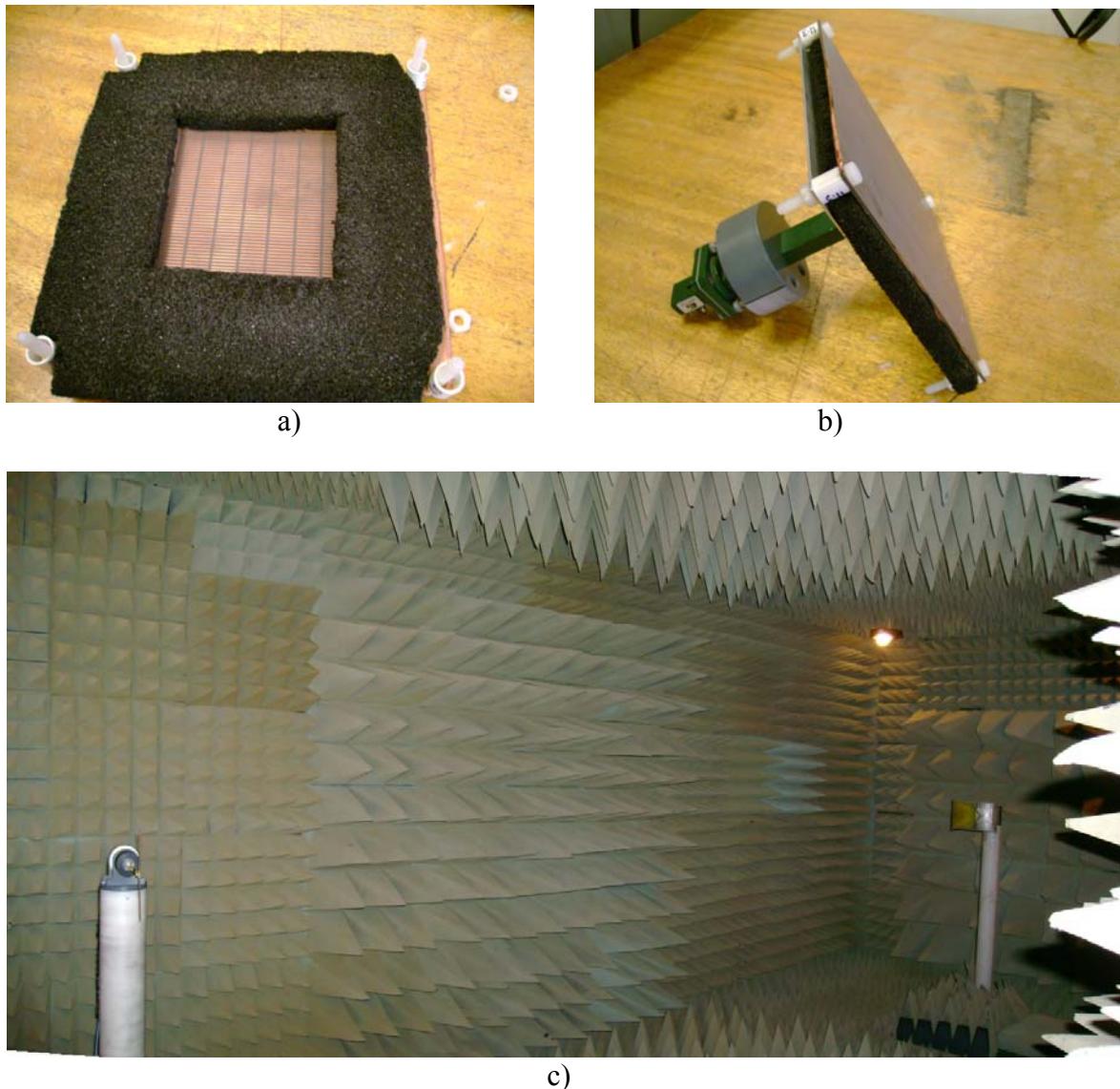
Figura 24. a) y b) Antena LW formada por una superficie periódica FSS de dipolos, rodeada por un material absorbente para evitar reflexiones y un plano de masa situado a cierta distancia de la FSS. **c)** Cámara anecoica donde se realizaron las medidas en anteriores experimentos. *Imágenes tomadas en el departamento de Ingeniería Electrónica y Eléctrica de la Universidad de Loughborough (Inglaterra).*

4   Conclusión

En este proyecto, se ha estudiado la aplicación de la Técnica de Resonancia Transversa para estructuras periódicas, actuando como Superficies Selectivas en Frecuencia, con el objetivo de obtener los Diagramas de Dispersión y Radiación de este tipo de antenas. Con el fin de resolver la función que define la Técnica de Resonancia Transversa, se ha implementado un programa en Matlab consistente en un método de búsqueda tanto de mínimos dependientes de una variable (caso Surface-Wave) como de mínimos dependientes de dos variables, en el plano complejo (caso Leaky-Wave), habiendo sido éste verificado con resultados de otros artículos y medidas reales. Los resultados obtenidos a lo largo de este proyecto han sido realizados para el modo TE, es decir, en el plano H, pero de la misma manera, cambiando las ecuaciones de las impedancias en el modelo equivalente, se podrían haber obtenido también para el modo TM, en el plano E. En este último caso, los resultados obtenidos no habrían sido tan precisos debido a que la periodicidad en el plano E es más grande, cercana a $\lambda/2$ y por esta razón, la superficie no se puede considerar como una admitancia homogénea a lo largo de toda la estructura, lo que constituye la teoría básica para aplicar un modelo equivalente para la Técnica de Resonancia Transversa.

Como una posible extensión del proyecto, se podría estudiar una estructura similar con múltiples capas. En este caso se podría realizar el mismo proceso que se ha seguido en este proyecto pero extendiendo el modelo equivalente de la celda unidad a una línea de transmisión con nuevas admitancias representando las capas de FSS. Sin embargo, en lugar de calcular el coeficiente de reflexión por medio del programa en Fortran basado en el método de los momentos para un análisis modal, se podría estimar usando las ecuaciones derivadas de una teoría general para interferómetros Fabry-Perot con multiespejos, donde cada una de las capas de nuestra estructura estaría representada por un espejo en dicha teoría. [4]

En futuros trabajos, sería interesante estudiar diferentes estructuras basadas en varias capas de FSS usando esta teoría como una posible mejora para el análisis de este tipo de antenas. También, interesaría profundizar en la teoría empleada en el cálculo de mínimos sobre dos dimensiones, como es el caso de las Leaky-Wave, mediante técnicas inteligentes de búsqueda de ceros en el plano complejos [18]

Para concluir, esta técnica ofrece un rápido y preciso método para conocer el comportamiento de una antena antes de su fabricación, que en general, ahorraría tanto tiempo como costes, factores tan importantes en cualquier organización. Por el contrario, se tendría que aplicar un proceso más complejo y lento como puede ser el análisis modal sobre toda la estructura, incrementando drásticamente el coste computacional con el número de capas de la estructura. Por esta razón, la aplicación del método implementado en este proyecto, ofrece una sencilla y rápida solución para la caracterización de este tipo de antenas compuestas por Superficies Selectivas en Frecuencia.

Actualmente, se ha escrito un artículo sobre el trabajo expuesto en este proyecto y está en trámites de ser presentado para una posible futura publicación.

Final Year Project Report

Analysis and Design of High Gain Planar Antennas.

Author: Cristina Arias Pérez (A620154).
Supervisor: Dr. Alexandros Feresidis.

Analysis and Design of High Gain Planar Antennas.

Cristina Arias Pérez.

Abstract— **In this project, a method based on a minimum search has been implemented in order to apply the Transverse Resonance Technique analysis and be able to calculate the Dispersion Diagram of Frequency Selective Surfaces (FSS) antennas. Three different structures have been studied and are presented in this report. All of them have one common characteristic: they are composed of periodic dipoles or tripoles patched surfaces but with different ways of operation, as surface-wave or leaky-wave antennas. The technique implemented has been verified by results found in different papers and measured data. The efficiency and quick solution of this method has been viewed as an advantage against other techniques, such as the modal analysis. This characteristic is a matter of vital importance in the study of multilayer structures in which a modal analysis for the whole structure would be complex to be executed.**

TABLE OF CONTENTS

I. INTRODUCTION

Frequency Selective surfaces, structures widely recognized for being used as filters for microwave and optical signals, are the basic topic of this report . These surfaces consist of periodic structures, represented through different distributions and forms, which will be studied in this section, and has multiple applications as improved antennas for modern wireless communication systems and in general in microwave engineering, obtained with low cost and simple fabrication.

Periodic structures refer to infinite transmission lines or waveguides loaded at periodic intervals with identical reactive elements. These can be either metallic patch elements or aperture elements within a metallic screen and exhibit total reflection (patches) or transmission (apertures) in the neighbourhood of the resonant element. Multiple kinds of periodic structures can be found depending on the shape of the reactive elements and their distribution in the surface, but in all cases it can be modelled as a reactance across a transmission line as it is shown in fig. 1. [6],[7]
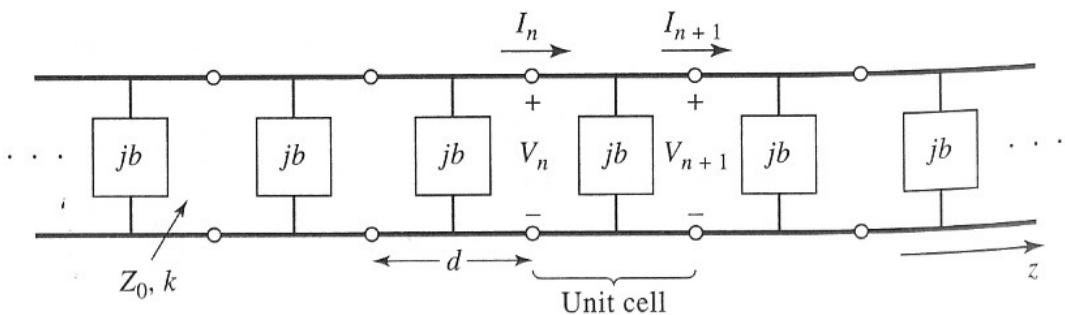

Fig. 1. Equivalent circuit of a periodically loaded transmission line. The unloaded line has characteristics impedance Z_0 and propagation constant k. [6]

All the periodic structures have two important properties in common, namely:
1. Passband-stopband characteristics.
2. Support of waves with phase velocities much less than the velocity of light. [7]

There will be passband in frequency bands where the wave propagates unattenuatedly and stop bands in frequency bands where the wave is cut off and does not propagate at all. The pass band-stop band property is of some interest for its frequency filtering aspects. The second property is of basic importance for travelling-wave tube circuits. In this kind of circuits, efficient interaction between the electron beam and the electromagnetic field is obtained only if the phase velocity is equal to the beam velocity, which is not greater than 10 to 20 percent of the velocity of light. Thus, considerable slowing down of the electromagnetic wave is required. Moreover, each FSS (Frequency Selective Surfaces) can be characterized by three factors: a) width of pass/stop band, b) band-edge ratio (-0.5dB- -10dB roll off rate), and c) stability of transmission response to angle of wave incidence. In general, due to the two main properties of these kinds of surfaces, FSS find application in travelling-wave tubes, masers, phase shifters, Leaky-Wave antennas, antennas for wireless networks and mobile communication base stations, satellite communication, sensors and car radars, etc. [7]

The Bloch theorem asserts that one wave is propagated in an atomic periodic structure as a plane wave which adopts the frequency and symmetry of the atomic structure, so the circuit analysis of a periodic structure involves studying an equivalent network for a single basic section (unit cell) of the original structure. This is followed by an analysis to determine the voltage and current waves that may propagate along the network consisting of the cascade connection of an infinite number of the basic networks.

A. Analysis of Infinite Periodic Structures.

The best way to calculate the transmission characteristics of a periodic surface is by using ABCD matrices. Each unit cell can be study separately, which consists basically of three two-port networks in cascade, and obtain its ABCD matrix multiplying the ABCD matrices representing each individual two-ports. It must be noted that the order of multiplication of the matrix must be the same as the order in which the networks are arranged, since matrix multiplication is not commutative.

In the case it is being studied, shown in Fig. 1, one unit cell is made up of a cascade of a transmission line section of length d/2, a shunt susceptance normalized b, and another transmission line section of length d/2 [6]. So the ABCD matrix for this unit cell in a normalized form is:

$$\begin{bmatrix} V_n \\ I_n \end{bmatrix} = \begin{bmatrix} A & B \\ C & D \end{bmatrix} \begin{bmatrix} V_{n+1} \\ I_{n+1} \end{bmatrix} = \begin{bmatrix} \cos\dfrac{\theta}{2} & j\sin\dfrac{\theta}{2} \\ j\sin\dfrac{\theta}{2} & \cos\dfrac{\theta}{2} \end{bmatrix} \begin{bmatrix} 1 & 0 \\ jb & 1 \end{bmatrix} \begin{bmatrix} \cos\dfrac{\theta}{2} & j\sin\dfrac{\theta}{2} \\ j\sin\dfrac{\theta}{2} & \cos\dfrac{\theta}{2} \end{bmatrix} \begin{bmatrix} V_{n+1} \\ I_{n+1} \end{bmatrix} \tag{1}$$

(The demonstration of the result of the ABCD parameters for one transmission line and admittance is developed in Appendix II).

Due to the fact that the structure is supposed to be infinitely long, it can be expressed as the following: $\begin{aligned} V_{n+1} &= V_n e^{-\gamma d} \\ I_{n+1} &= I_n e^{-\gamma d} \end{aligned}$. Then, (1) can be rewritten as:

$$\begin{bmatrix} A - e^{\gamma d} & B \\ C & D - e^{\gamma d} \end{bmatrix} \begin{bmatrix} V_{n+1} \\ I_{n+1} \end{bmatrix} = 0 \tag{2}$$

For a nontrivial solution, the determinant of the above matrix must vanish and since AD-BC=1 (characteristic of reciprocal networks), the following solution can be obtained easily ([6], p.425):

$$\cosh \gamma d = \cosh \alpha d \cos \beta d + j \sinh \alpha d \sin \beta d = \cos\theta - \frac{b}{2}\sin\theta \tag{3}$$

As it can be observed, the right part of the expression is real so α or β must be zero.

a) If α=0 and β≠0, then the passband case of the structure occurs because wave is nonattenuated.

b) If α≠0 and β=0, then the stopband case of the structure occurs because wave is attenuated.

B. Techniques of Analysis

[1] Basically, three ways may be chosen to calculate transmission characteristics of FSS. These ways are based on: empirical methods by measuring the surface to study, modal analysis, and equivalent circuits.

1) Empirical Methods:

This method consists in the execution of some measurements for different shapes and distribution of the reactive elements in the surface. Once they have been carried out, they are compared in order to obtain accurate results. It is based on experience.

2) Modal Analysis

[1] The basic of this method is the analysis of the electromagnetic fields that occur to the structure. The first thing to do in formulating the problem of electromagnetic scattering from a FSS is to relate the fields scattered from the FSS to the surface currents induced on the screen by the incident field. To do it easier, at the beginning it can be assumed that the FSS is infinitesimally thin, valid for most applications, although later equations must be modified to handle an FSS on a dielectric substrate, and with a finite conductivity.

This relation is expressed as follows:

$$\begin{bmatrix} A_x(x,y) \\ A_y(x,y) \end{bmatrix} = \overline{\overline{G}}(x,y) * \begin{bmatrix} J_x(x,y) \\ J_y(x,y) \end{bmatrix} \qquad (4)$$

Where J refers to the surface current density induced on the FSS and A to the magnetic vector potential due to this current.

The expression for $\overline{\overline{G}}$ is the following:

$$\overline{\overline{G}} = \frac{\exp(-jk_0 r)}{4\pi r} \overline{\overline{I}},$$

$$r = \left(x^2 + y^2\right)^{1/2},$$

$k_0 =$ Free-space wave number,

$\overline{\overline{I}} =$ Identity tensor, and $*$, the convolution operator.

The following step in modal analysis is to express the transverse components of the scattered electric field E_s in the plane of the screen

$$
\begin{bmatrix} E_x^s \\ E_y^s \end{bmatrix} = \frac{1}{jw\varepsilon_0} \begin{bmatrix} \dfrac{\partial^2}{\partial x^2} + k_0 & \dfrac{\partial^2}{\partial x \partial y} \\ \dfrac{\partial^2}{\partial x \partial y} & \dfrac{\partial^2}{\partial y^2} + k_0 \end{bmatrix} \begin{bmatrix} A_x \\ A_y \end{bmatrix} \tag{5}
$$

In order to take advantage of the periodicity of the geometry, (5) is rewritten in the spectral domain using the Fourier transform:

$$
\begin{bmatrix} E_x^s(\alpha,\beta) \\ E_y^s(\alpha,\beta) \end{bmatrix} = \frac{1}{jw\varepsilon_0} \begin{bmatrix} k_0 - \alpha^2 & -\alpha\beta \\ -\alpha\beta & k_0 - \beta^2 \end{bmatrix} \overline{\overline{\widetilde{G}}}(\alpha,\beta) \begin{bmatrix} J_x(\alpha,\beta) \\ J_y(\alpha,\beta) \end{bmatrix} \tag{6}
$$

Where:

$$
\overline{\overline{\widetilde{G}}}(\alpha,\beta) = \frac{-j}{2\left(k_0^2 - \alpha^2 - \beta^2\right)^{1/2}} \overline{\overline{I}} \, ,
$$

And α and β are the transform variables corresponding to the x and y coordinates, respectively.

Once the induced currents have been determined, other quantities of practical interest, e.g., reflection and transmission coefficients for the dominant harmonics, as well as the scattering matrix description for the screen, can be calculated.

In order to solve the equations, the *Moment Method* is used. The efficiency in solving with this method depends critically upon the choice of the basis functions. It is helpful to consider several factors in choosing these functions: 1) it is advisable that the number of basis functions used to represent the unknown current be minimal, and therefore the matrix size be small, 2) it is convenient to choose the basis functions that are analytically Fourier transformable, 3) the transforms of the basis functions must decay rapidly for large α and β in order to reduce the computing cost solving the scalar products that appear in the matrix elements, 4) it must be taken into account that if the number of basis functions needed becomes too large for the core memory of the computer, then a solution scheme that is different from the Gaussian elimination method, such as an iterative procedure, should be utilized.

Basically two kinds of basic functions can be used to represent the unknown functions when the Moment Method is applied: the *entire domain* and *subdomain* basis functions. The first ones span the entire support of the unknown, the patch or the aperture in a FSS cell, and are typically tailored for the specific geometry of the region over which the unknown is being expanded. The most important advantage of using the entire domain kind of basis functions is that it has a much smaller Moment Method matrix than that used in subdomain functions. Nevertheless, for an arbitrary patch or aperture geometries, entire domain basis functions are not available in general. Consequently, for working with FSS screens composed of arbitrarily/shaped apertures or patches, and for screens with finite conductivities, subdomain basis functions have been found to be more versatile than the entire domain functions.[1]

3) Equivalent circuits

An alternative technique to the Floquet modal analysis, before having such powerful computers, was the use of equivalent circuit models to find Electromagnetic Band Gap (EBG) characteristics for the structure in study. These are still strongly useful to establish in a quick way whether or not an FSS could provide a solution to an immediate design problem. They are scalar empirical models, derived by fitting to experimental transmission or reflection coefficients measured as functions of frequency, and consequently a separated model is required for each individual element.

As a simple example it will be used the circuit model studied in [5] that describes the free/standing infinite array of conducting patches shown in Fig. 2. In this figure, the equivalent circuit is also described for a unit cell of this distribution.

The inductance represents the currents induced on the array of elements. The capacitance represents the electric fields between successive elements as well as fringing fields. In [5], it is deduced that as the patches move closer, the distance between opposite gathering charges at the edges of successive patches is reduced. Thus, the equivalent capacitance is increased. On the contrary, the total equivalent inductance of the equivalent circuit in Fig. 2 is reduced in the same way as does the periodicity. In fact it is demonstrated that the relative reduction of the inductance with periodicity is more significant than the relative increase in capacitance. This offers a good explanation of the fact that the resonant frequency $\left(w = \dfrac{1}{\sqrt{LC}} \right)$ of such arrays increases as the elements are packed more closely.
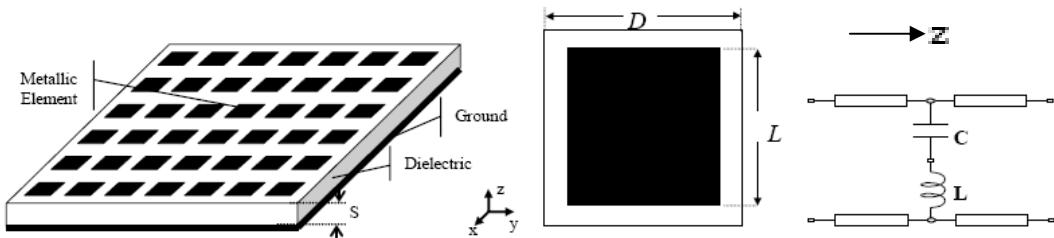

Fig. 2. Layout of the structure under investigation (top). Unit cell and equivalent circuit for square patch array (bottom).[5]

The equivalent circuit of the layout shown in Fig. 2 can be described with a short circuited termination representing the ground plane, as shown in Fig. 3:
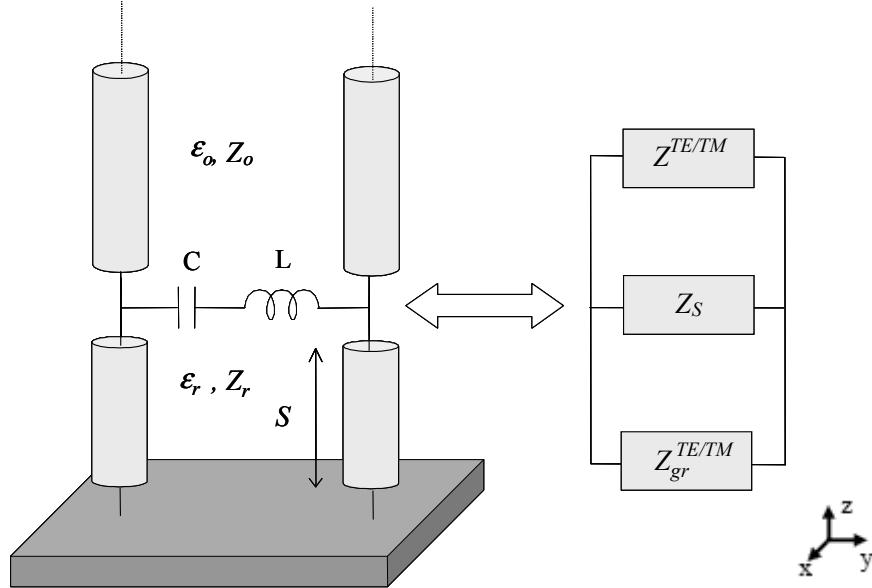

Fig. 3. Equivalent network of the capacitive screen over a grounded dielectric slab.[5]

This circuit is used to calculate in a quick way an approximation of the bandgap frequency for the structure represented in Fig. 2, by using the *Transverse Resonance Technique.*

This technique consists in employing a transmission line of the transverse cross section of the waveguide, and gives a simple and direct solution for the cutoff frequency. Once this frequency is known, the propagation constant in the z axis of the guide (according to our reference system) may be determined using the following equation [3]:

$$k_z = \sqrt{k^2 - k_c^2} \qquad (7)$$

Where $k_c = \sqrt{k_x^2 + k_y^2}$ is the cutoff wave number of the guide and $k = \varepsilon_r k_0$, where ε_r is the dielectric's relative permittivity.

This method is based on the fact that in a waveguide at cutoff, the fields form standing waves in the transverse plane of the guide. This situation can be modelled with an equivalent transmission line circuit operating at resonance. One of the conditions of such a resonant line is the fact that, at any z point on the line, the sum of the input impedances seen at either side must be zero. That is:

$$Z_{in}^r(z) + Z_{in}^l(z) = 0 \text{, for all z.} \qquad (8)$$

Then, for the equivalent circuit in Fig.3, the Transverse Resonance Technique function would be written as follow:

$$\frac{1}{Z_S} + \frac{1}{Z_0^{TE/TM}} + \frac{1}{Z_{gr}^{TE/TM}} = 0 \qquad (9)$$

This is the same expression than (8) because the different elements of the transmission line in z axis (Z, Z_s and Z_{gr}) are located in parallel through it. Therefore, it is very easy to work with admittances.

Where:

$$Z_S = jwL + \frac{1}{jwC}, Z_0^{TE} = \frac{w\mu_0}{k_{z_0}} \text{ and } Z_0^{TM} = \frac{k_{z_0}}{w\varepsilon_r\varepsilon_0}, \text{ for propagation in z direction.}$$

ε_0 and μ_0 the permittivity and permeability of free space and ε_r the dielectric constant of the medium where the wave propagates. The ground plane is transferred along the finite thickness of the dielectric substrate and is expressed as:

$$Z_{gr}^{TE/TM} = jZ^{TE/TM} \tan\left(k_{z_{gr}} s\right) \text{ (short-circuited line case).}$$

Where: $Z^{TE} = \frac{w\mu_0}{k_{z_{gr}}}$ and $Z^{TM} = \frac{k_{z_{gr}}}{w\varepsilon_r\varepsilon_0}$.

(Note that the general expression for input impedance is:

$$Z_{in} = Z_{line} \frac{Z_{load} + jZ_{line} \tan\left(k_{zline}s\right)}{Z_{line} + jZ_{load} \tan\left(k_{zline}s\right)}, \text{ and for a short-circuited line case } Z_{load} = 0 \text{).}$$

An other important condition used in this technique is obtained from the fact that the propagation constant in transversal direction to z axis, k_c, must be the same in all the regions for phase matching of the tangential fields at the dielectric interface. Thus, with k_x=0, for the structure in Fig. 2 it can be written:

$$k_y = \sqrt{\varepsilon_r k_0^2 - k_{z_{gr}}^2} \, (dielectric) = \sqrt{k_0^2 - k_{z_0}^2} \, (air) \qquad (10)$$

Equations (9) and (10) can be used finally to obtain the transversal constant propagation which will allow us to build the Dispersion Diagram of the structure (k_y vs. f (GHz)). It must be taken into account that transverse resonance technique only gives results for the cutoff frequency of the guide. If fields or attenuation due to conductor losses are needed, the complete field theory solution will be required.

The aim of the Project has been the analysis of FSS using the Transverse Resonance Technique, for three different structures, by using equivalent circuits or the values of the

susceptances which represent the surfaces; for the last structure the susceptance was calculated through a software whose main work operating is based on the modal analysis explained in the A. 2) section of this Introduction. Nevertheless, the complex task to analyze this last structure has been reduced due to the fact that the modal analysis introduced by the software has been only used to calculate the admittance of a single FSS, but not the whole structure. This analysis has been carried out in order to get accurate results for Dispersion Diagrams and Radiation Patterns for the H-plane in a quick and easy way. Moreover, as a possible widening of the project presented in the Conclusion section of this report, the technique implemented for the case of one layer is also applied for the case of multilayer by knowing the total reflection coefficient of the structure. The total modal analysis for multilayer is very complex, so the method implemented in this project is a matter of vital importance in this field for the characterization of antennas.

II. APPLICATIONS

A. Surface Waves

In this section of the report, one structure is going to be studied for a surface-wave antennas operation. Surface-wave antennas are purely end-fire antennas (see Fig. 4). The basic guiding structure for surface-wave antennas is an open waveguide whose dominant mode (the surface wave) is purely bound, so that the surface wave will radiate only at discontinuities, such as at very end of the waveguide.

It does not radiate along the length of the guide because the surface wave is a slow wave, i.e. $\beta > k_0$, being k_0 the free space wave number in air, (except for some small leakage into the almost-end-fire direction if the surface-wave antenna is tapered). The wave number (or propagation constant) is, in this case, real, and composed only of a phase constant, $k_p = \beta$.
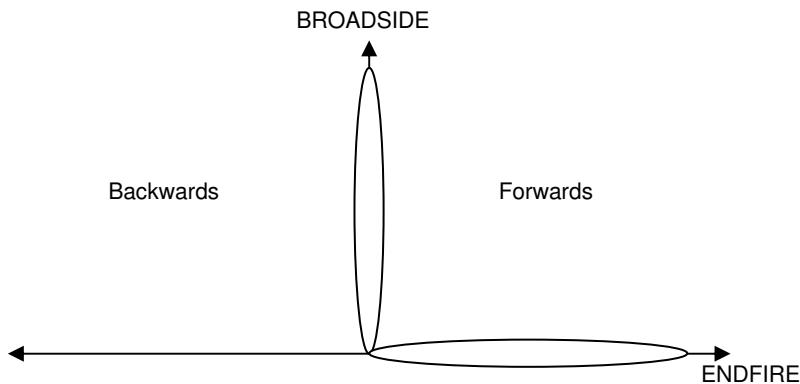
Fig. 4. Antennas directions. Endfire corresponds with the direction on the antenna plane and Broadside corresponds with the perpendicular direction to the antenna plane.

1) Structure 1:

The first structure to study is the one presented in Fig. 5 a). This structure, composed of tripole elements, is used in [3] as a Miniaturized Electromagnetic Band Gap structure (MEBG) for mobile applications, essential for applications in terminal handheld devices. As MEBGs are composed of resonant elements, the dimension of each element is about half a wavelength so for devices operating at high frequencies, a miniaturization must be required for its integration in modern handheld terminals.
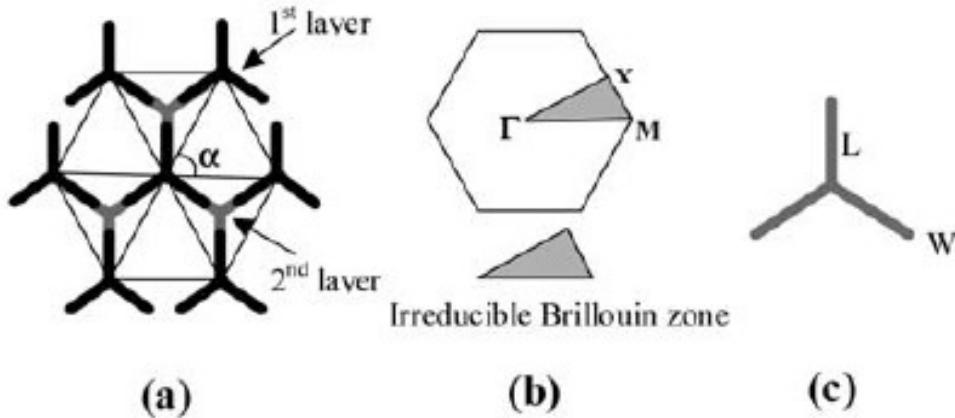
Fig. 5. a) Direct lattice, **b)** reciprocal lattice and its irreducible Brillouin zone, and **c)** tripole dimensions L=5mm, W=0.5 mm, periodicity D=12mm, ε_r=2.2, thickness s=1.13mm, and α=60°. [3]

The aim for this structure is to get the dispersion diagram from the equivalent circuit of the structure by using the Transverse Resonance Technique.

As shown in Fig. 6, the equivalent circuit for one unit cell of the surface consists of two transmission lines (which represent the air), a capacitance and an inductance. The structure is free standing so the transmission lines can be considered infinites, with $\varepsilon_r = 1$.
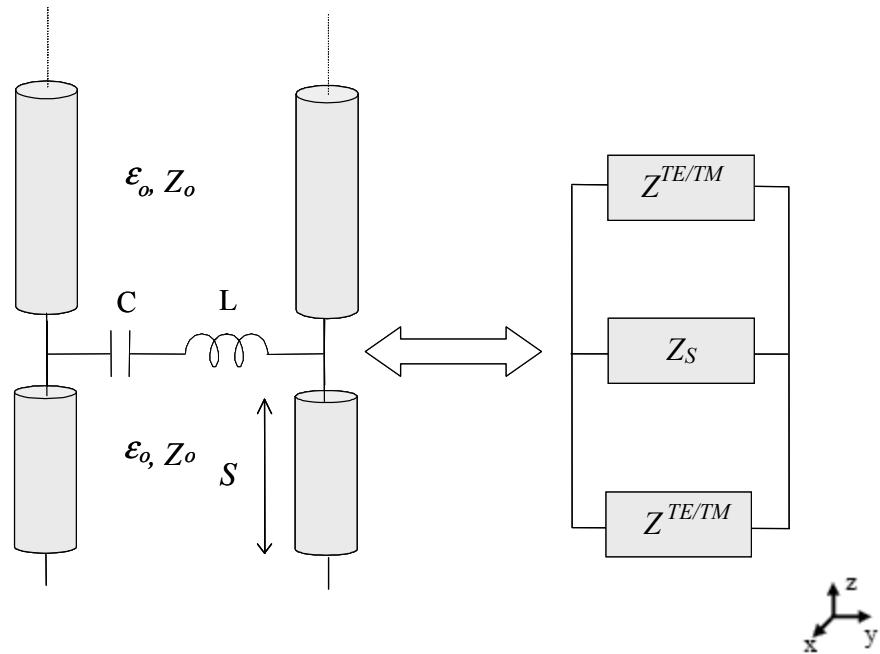
Fig. 6. Equivalent circuit of an unit cell for the structure shown in Fig. 5.

When applying the Transverse Resonance Technique studied in the Introduction section, the following equation is derived from (9):

$$Y_s + 2 \cdot Y_0 = 0 \qquad (11)$$

44

Where:

$Y = \dfrac{1}{Z}$ (in general).

$Z_s = jwL + \dfrac{1}{jwC}$, and

$Z_0^{TE} = \dfrac{k_0 \cdot \eta_0}{k_z} = \dfrac{w \cdot \mu_0}{k_z}$, (it is going to be studied only the TE case).

In order to get an analytical solution for the propagation constant in the y axis direction (supposing no propagation in x axis), (7) and (11) are used.

The final analytical solution is the following:

$$k_{TE} = \frac{w}{c}\sqrt{1 + 0.25\left[\frac{wC\eta_0}{1 - \left(\dfrac{w}{w_0}\right)^2}\right]^2} \qquad (12)$$

Where η_0 represents the free space wave impedance and $w_0 = 1/\sqrt{LC}$, is the resonant frequency of the series LC circuit representing the array. (See development in Appendix II).

This analytical solution was applied in a Matlab code to get the Dispersion Diagram for L=2nH, C=0.41pF (case of a thick structure, W=5mm) and C=13.28pF (case of a thin structure used as miniaturized, W=0.5mm) of the first TE mode for the ΓM direction. The dispersion diagram of both cases plotted in Matlab is the one represented in Fig. 7.
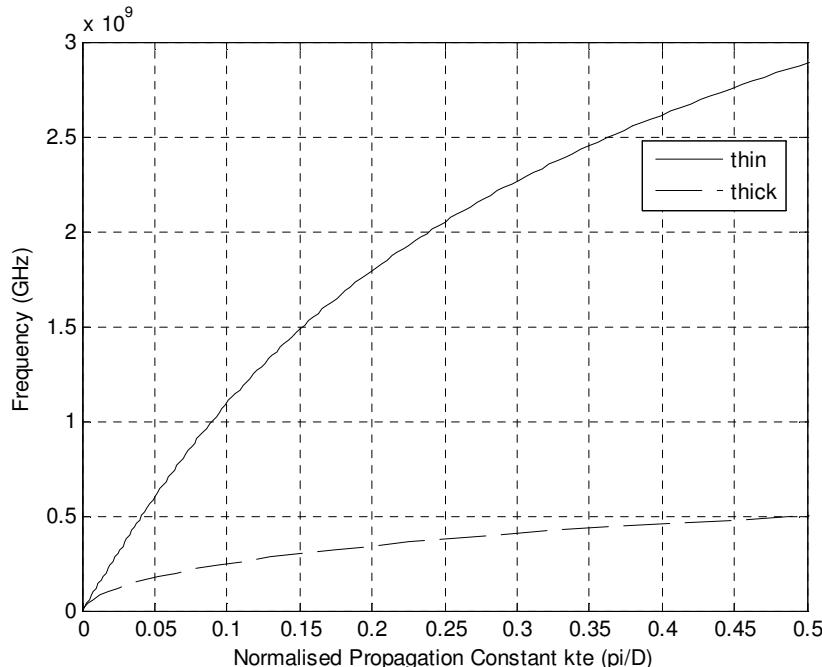
Fig. 7. Dispersion diagram for thin and thick tripoles. Analytical solution.

For this simple case in which it is supposed free-standing, without either dielectric or ground plane, it was easy to get the analytical solution for the propagation constant. Although in the case in which there is a ground plane, an analytical solution can not be calculated due to the tangent element of Z_{gr} in (9). For this reason, in this project, an efficient and quick method has been implemented to get an accurate solution for the propagation constant. This method consists in calculating the value of the propagation constant that makes minimum the function (9) in general, or (11) for the structure in this section. First of all, a range of values for the propagation constant is given, taking into account that this structure is being studied as a Surface-Wave antenna so the propagation constant must fulfil that $k_y = \beta > k_0$. Then, all the possible values in the range for k_y are applied to the equation (11) which defines the Transverse Resonance Technique for a specific frequency. Finally, the solution for this frequency is the value of k_y which makes minimum the absolute value of the function. Figures 8 and 9 shown a visual example for the minimum search method applied to the absolute value of the function (11), for a frequency of 0.5GHz.
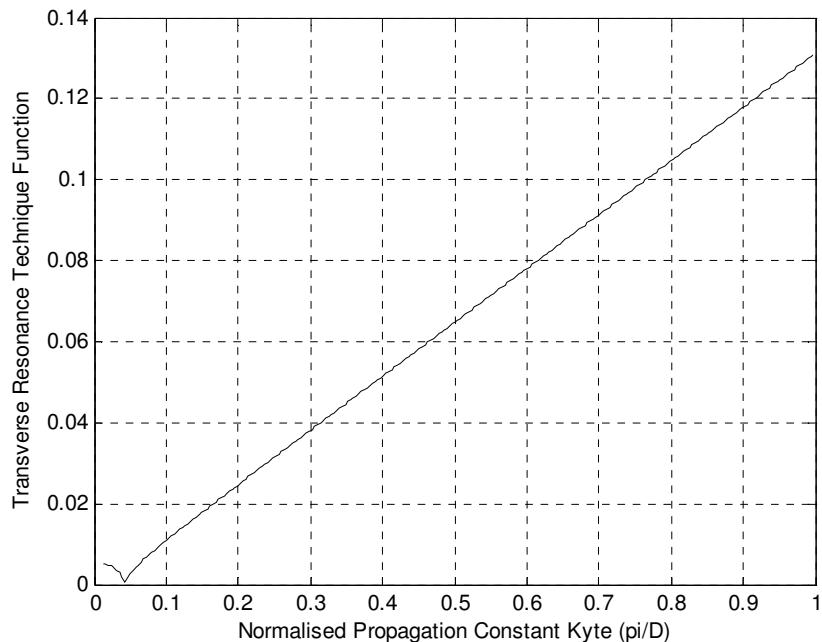

Figura 8. Thin tripoles case. **Absolute value** of the Transverse Resonance Technique function, (11), against $k_y=\beta$ for f=0.5GHz.

46
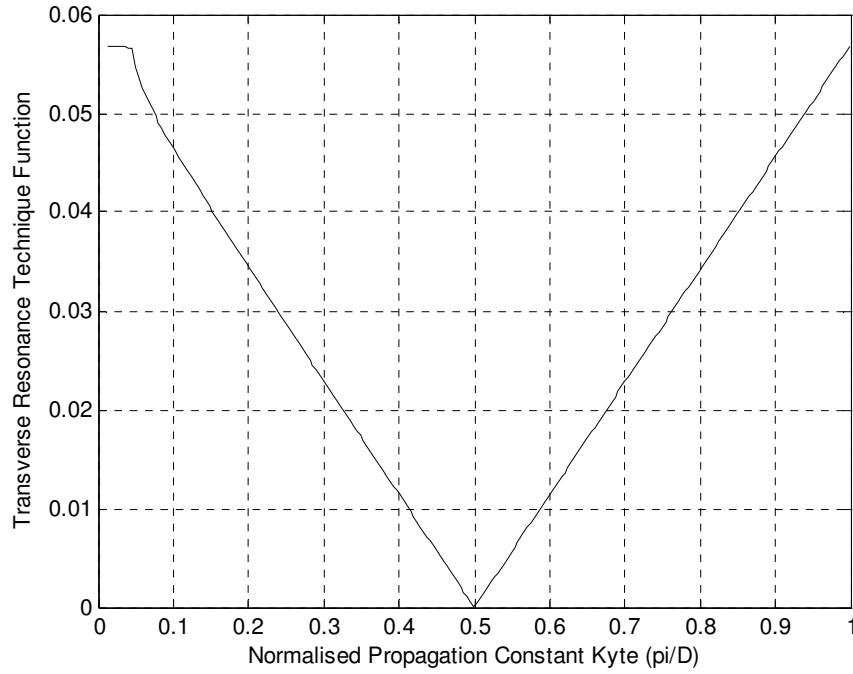
**Figura 9.** Thick tripoles case. **Absolute value** of the Transverse Resonance Technique function, (11), against $k_y=\beta$ for f=0.5GHz.

Furthermore, when k_z is calculated as (7), a positive and imaginary value for k_z is obtained, which means that the attenuation constant in z direction would be negative. Note that the expression should be in the form $k_z = -j\alpha$. As it has no sense for surfaces waves in z direction, in order to get the right solution the negative solution of the root must be taken instead of the positive one. In later structures, in the study of leaky-waves, the positive solution of the root must be taken in a case of forward propagation, due to the fact that the contribution of the other cells makes an increase of energy in z direction, i.e. attenuation constant is negative. For more details about this phenomenon, see [19].

In order to compare the solution obtained with this new method and a real one, this first simple structure has been studied. Fig. 10 shows the solution with the Minimum Search method. As it can be observed, similar solutions have been obtained; hence, the method implemented in this project has been verified.

The code for the Minimum Search method applied for this structure is attached in Appendix II.
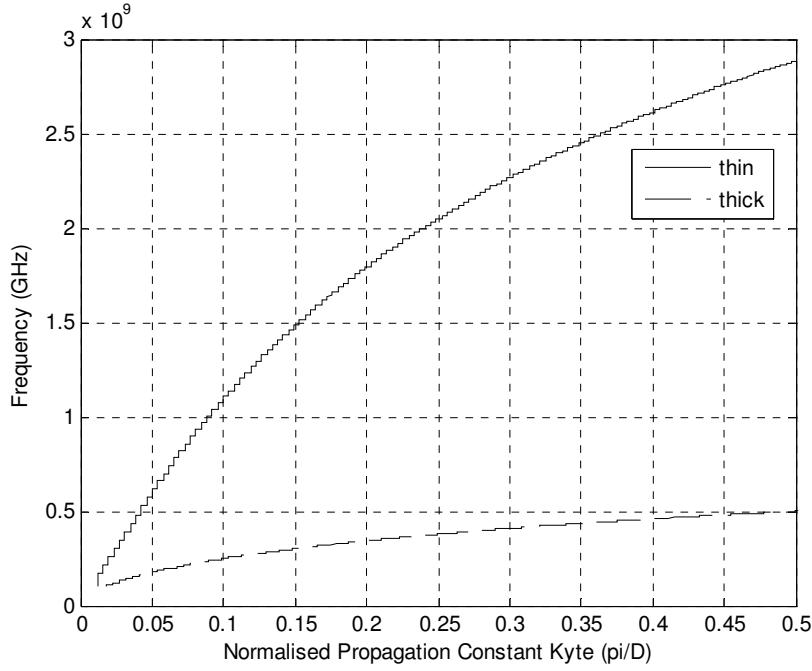
Fig. 10. Dispersion diagram for thin and thick tripoles. Minimum Search method solution.

B. Leaky Waves

In this section, two different structures will be studied for a periodic leaky-wave antennas operation. Planar leaky wave antennas are attractive due to their structural simplicity, easy fabrication, and integration with other planar components. Periodic leaky-wave antennas are often based on surface waveguides. There the basic waveguide can be an open structure whose dominant mode is a surface wave that is a slow wave, and the radiation is produced by placing a periodic array of discontinuities on the guide in such a way that the first space harmonic becomes fast, i.e. $\beta < K_0$, consequently it radiates. [14]

Leaky wave antennas do not radiate well in the end-fire direction and, in fact, are designed either to radiate in some other direction or to scan over a range of angles. The intention in the leaky-wave antennas is to produce a slow leakage per unit length; thus, each discontinuity element in the periodic array of elements produces a small loading on the basic waveguide mode. The individual elements are intentionally made nonresonant. As a result, the design procedure views the leaky-wave antennas as an equivalent homogeneous structure with a complex propagation wave number, $k_p = \beta_p - j\alpha_p$, where the array of discontinuity elements is considered as a whole in the analysis. Therefore, the wave number is composed of a leakage constant, α, and a phase constant, β; α is large or small depending on whether the leakage per unit length is large or small. A large α implies that the large leakage rate produces a short effective aperture, so that the radiated beam has a large beamwidth. Conversely, a low value of α, results in a long effective aperture and a narrow beam, provided the physical aperture is sufficiently long. One tries to design a leaky-wave antenna so that its value of α allows about 90 percent of the power in the guide

48

to be leaked away (radiated) by the time the wave reaches the end of the antenna aperture. Another characteristic to take into account is that because the phase constant β changes with frequency, so does the beam direction and, in general, the leaky-wave antenna can be scanned by varying the frequency. [14]

1) Structure 2:

The following structure to study corresponds to the one presented in [15]. The equivalent network of this structure is shown in Fig. 11. Hence, from this equivalent network, the Transverse Resonance Technique can be easily applied.

For this structure, S=5mm, $\varepsilon_r = 2.2$, $\mu_r = 1$, and $\overline{B}_s = 20$ is the susceptance which represents the FSS (imaginary part of the admittance) where the bar means normalization by multiplication with the free-space characteristic impedance η_0.
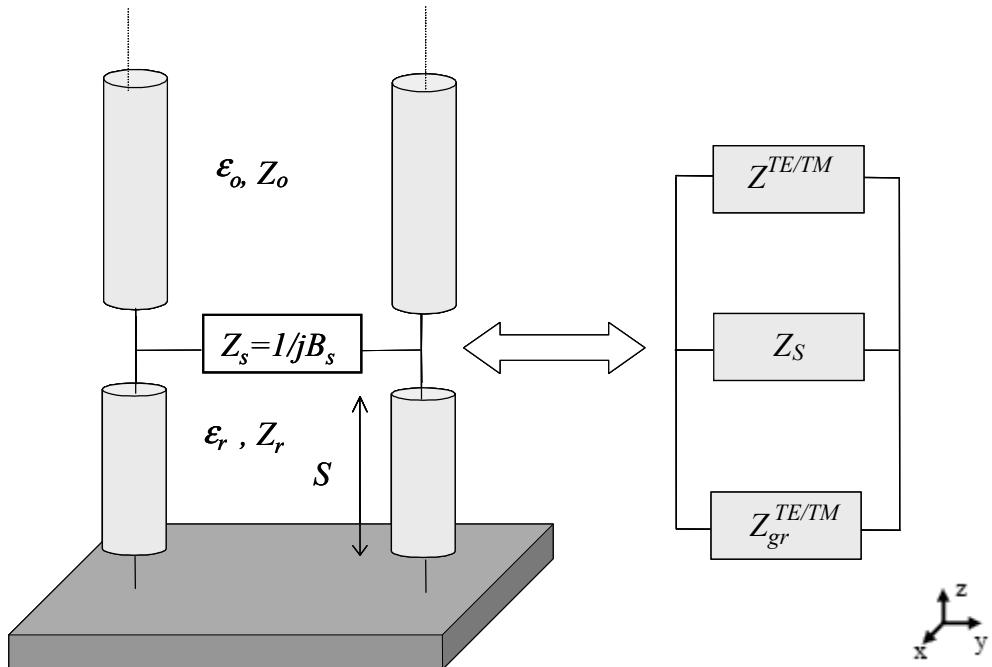
Fig. 11. Equivalent network over a grounded dielectric slab.

The Transverse Resonance Technique function for this structure is the following:

$$Y_S + Y_0^{TE} + Y_{gr}^{TE} = 0, \qquad (13)$$

Where:

$$Y_S = j\overline{B}_S, \quad Y_0^{TE} = \frac{k_{z_0}}{k_0\eta_0} = \frac{k_{z_0}}{w\mu_0} \quad \text{and} \quad Y_{gr}^{TE} = -j\frac{k_{z_{gr}}}{k_0\eta_0\mu_r}\cot\left(k_{z_{gr}}S\right).$$

In order to calculate k_y from k_z in the Matlab code, k_z is replaced by using (7) in the corresponding equations of the admittances.

The difference with the first structure is that now, the relevant TE leaky mode supported by this structure is being studied, so two parameters, α and β, must be taking into account in order to look for the minimum of the Transverse Resonance Technique function. With this aim, a range of values for α and β have been chosen and all the possible combinations of these two parameters have been applied in the function. Finally the combination which makes minimum the function for each frequency is the solution to find for that frequency. As a visual example of this minimum search in the complex plane, Fig. 12 shows in three dimensions the absolute value of the function (13) against α and β for a frequency of 20.8GHz.
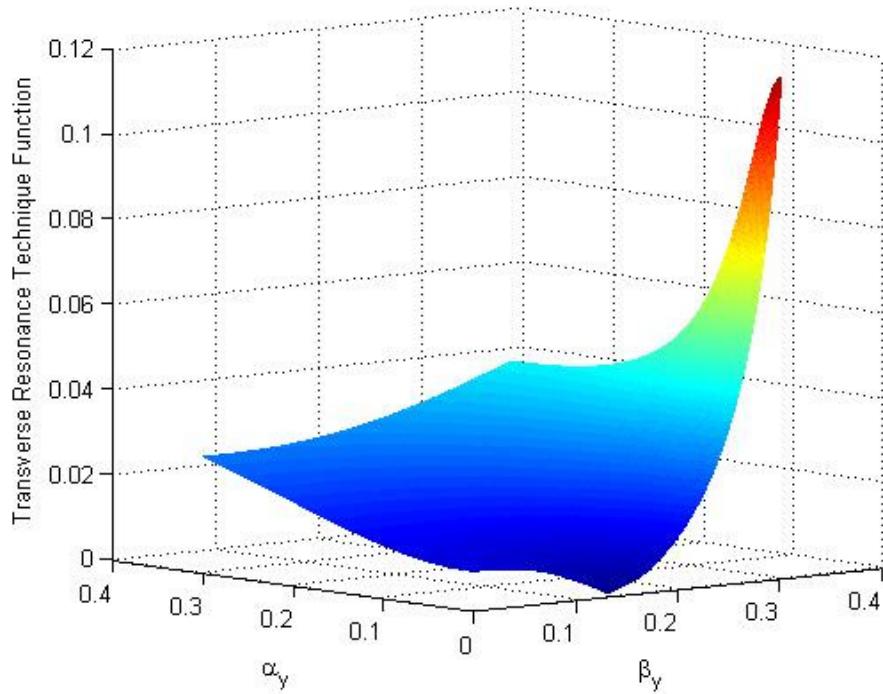
Fig. 12. Three dimensions plot. **Absolute value** of the Transverse Resonance Technique function, (13), against β and α for f=20.8GHz.

Applying the Minimum Search method for (13) to the whole range of frequencies, the results obtained are the following:
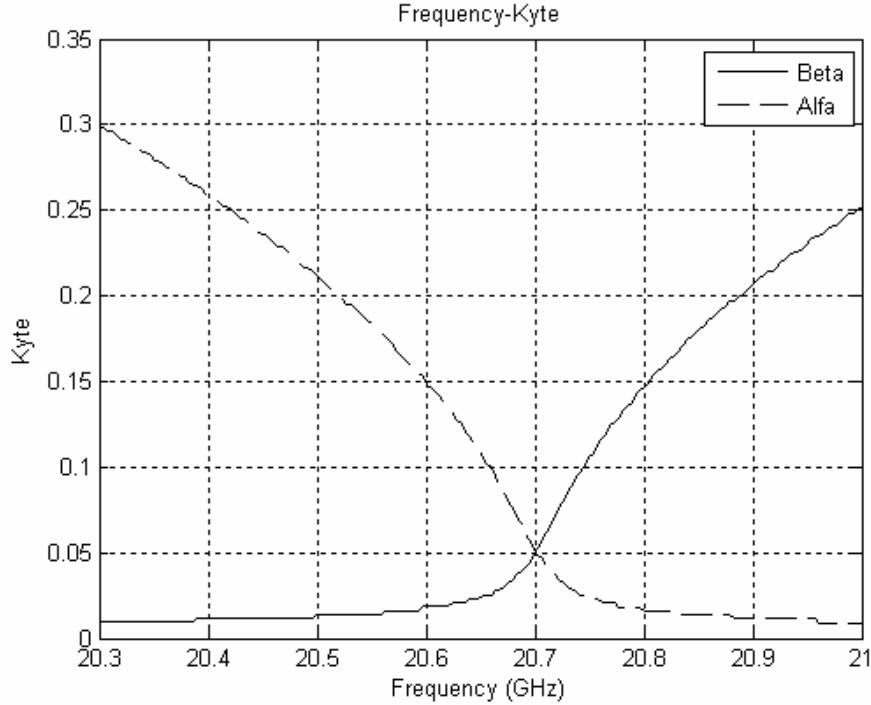
**Fig. 13.** Normalized leaky-wave phase ($\hat{\beta}$) and attenuation ($\hat{\alpha}$) constants as a function of frequency f for the relevant TE leaky mode of a LWA antenna. Parameters: S=5mm, $\varepsilon_r = 2.2$, $\mu_r = 1$, and $\overline{B}_s = 20$.

As it can be observed, similar results to the ones in [15] have been obtained by using the method implemented in this project, which verify once more this technique.

The condition α =β represents the sought splitting condition between the case of a beam pointing exactly at broadside (when β< α) and a beam with two peaks close to, but off, broadside (when β> α). Note that: $\sin(\theta_0) \approx \dfrac{\beta}{k_0}$, where θ_0 is the angle of the maximum of the beam (maximum radiation), measured from the broadside direction, as shown in figure 14.
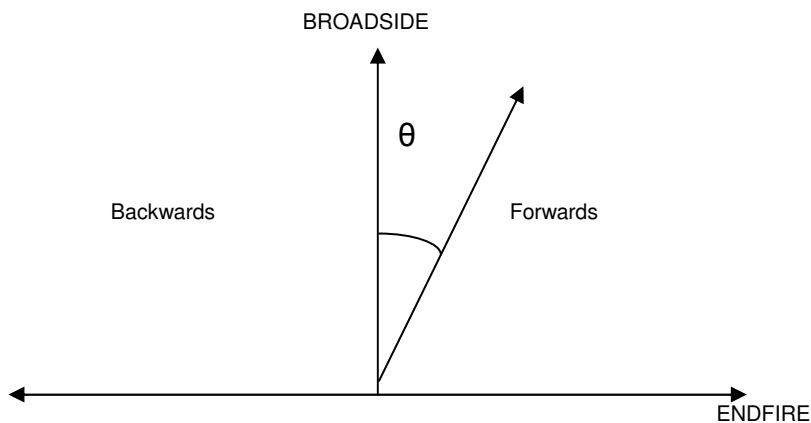

Fig. 14. Antennas directions. Endfire corresponds with the direction on the antenna plane and Broadside corresponds with the perpendicular direction to the antenna plane. θ represents the scanned angle of the antenna.

51

2) Structure 3:

  a)   Leaky-Wave Analysis.

The structure represented in Fig. 15. covers the most important study of this project. It consists of a periodic dipoles surface suspending in air, creating a distance S from the ground plane, i.e a semi-infinite transmission line. For the previous structures, the possibility of getting the Dispersion Diagram was achieved thanks to an equivalent circuit or and admittance given for a specific FSS. In this structure, a Fortran program (Appendix I) was used in order to calculate the admittance of the corresponding FSS (Fig. 16.).
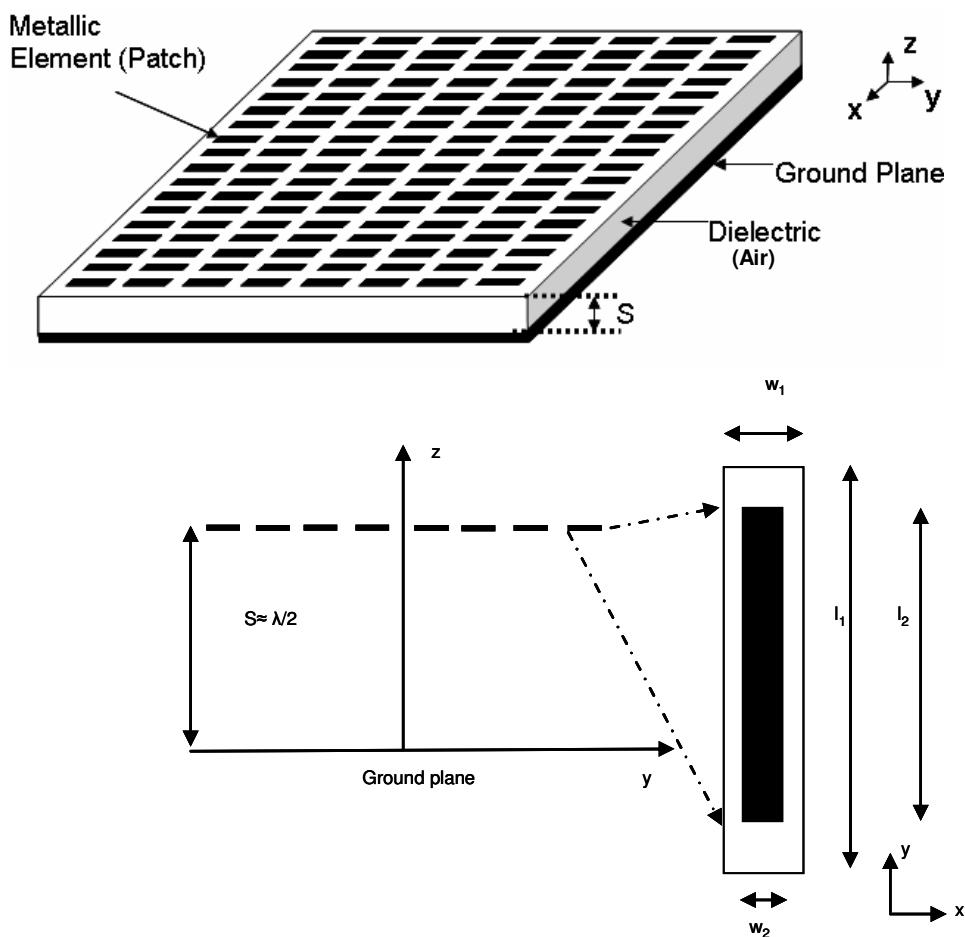
Fig.15. Schematic diagram of the leaky-wave antenna and detail for the structure's unit cell. Data: w_1=1 mm , w_2=0.5 mm, l_1=14.5 mm, l_2=14 mm, and S=h=11 mm .[16]

The result of the Fortran code gives the reflection coefficient of the FSS for each frequency studied, and these are used to calculate the admittance of the surface. These values are calculated in the Fortran program for a FSS suspended at an interface between air (above) and air (below), i.e. infinite lines in both sides (Fig. 16). Because of this fact, the admittance of the surface can be easily obtained from the following equation:

$$\Gamma = \frac{Z_{in} - Z_0}{Z_{in} + Z_0} \qquad (14)$$

Where Γ is the reflection coefficient seen at the arrow in Fig. 16, Z_{in} the input impedance seen at the same point, and Z_0 the characteristic impedance of the transmission lines.
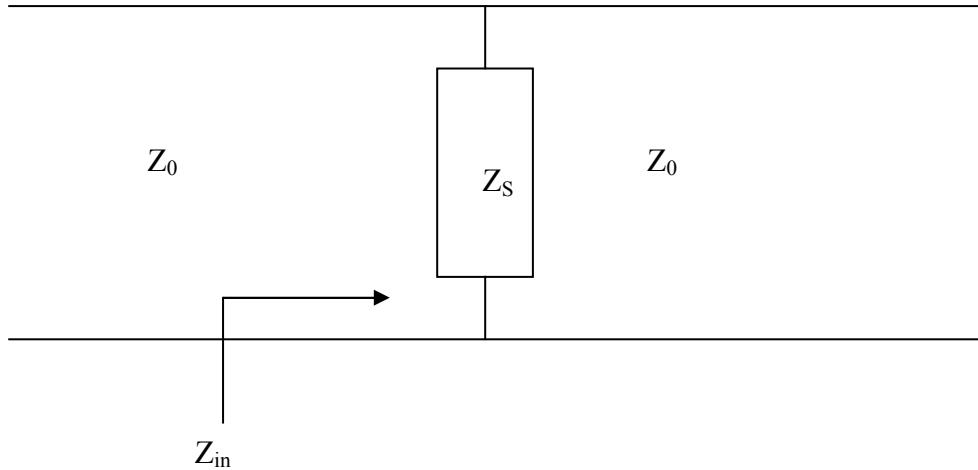

Fig. 16. Equivalent Network for the ideal case where the transmission lines are infinites (FSS suspended in the air) in Fortran Program. Z_S is the impedance of the FSS.

As the "transmission line" is infinite, Fig. 16 can be modified to Fig. 17 and then, a case of parallel impedance is easily solved. Equation (14) is rewritten as follows:

$$\Gamma = \frac{Z_S // Z_0 - Z_0}{Z_S // Z_0 + Z_0} \qquad (15)$$

Where $Z_S // Z_0$ refers to the result of the parallel impedance of Z_S and Z_0. Solving (15) and knowing that the admittance is the inverse of the impedance, the result for Y_S is the following:

$$Y_S = -\frac{2\Gamma}{Z_0(1 + \Gamma)} \qquad (16)$$
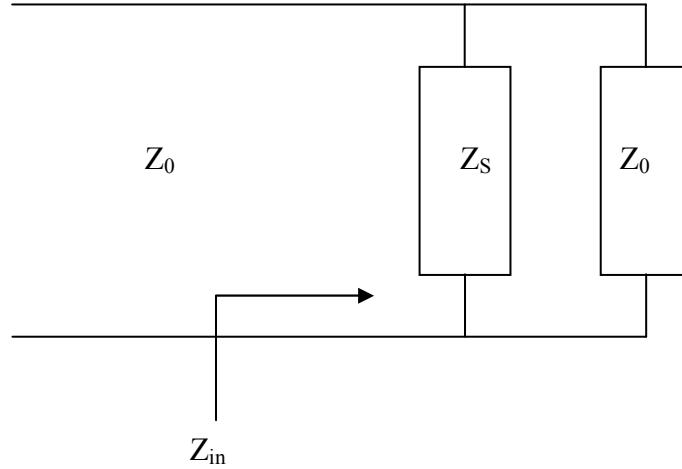
. **Fig. 17.** Equivalent Network derived from Fig. 13, due to the fact that the transmission line at the right side of Z_S is infinite.

Once the admittance of the FSS has been calculated, the Transverse Resonance Technique can be applied from the equivalent network of the total structure shown in Fig. 18. The function in this case is expressed as follows:

$$Y_S + Y_0^{TE} + Y_{gr}^{TE} = 0 \qquad (17)$$

Where:

Y_S is the result of (16), $Y_0^{TE} = \dfrac{k_{z_0}}{k_0 \eta_0} = \dfrac{k_{z_0}}{w\mu_0}$ and $Y_{gr}^{TE} = -j\dfrac{k_{z_0}}{k_0 \eta_0}\cot\left(k_{z_0} S\right)$.
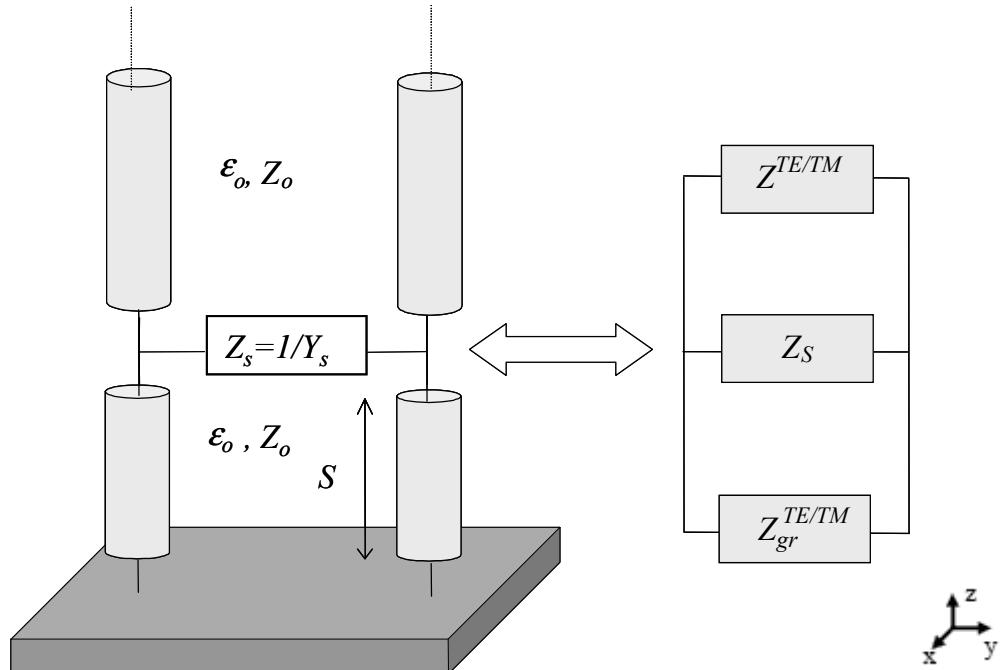

Fig. 18. Equivalent Network of the structure presented in Fig. 12.

In order to calculate k_y from k_z in the Matlab code, directly, k_z is replaced by using (7) in the corresponding equations of the admittances.

Once all the data to calculate the Dispersion Diagram are available, the Minimum Search method is applied and the solutions obtained are the following, shown in Fig. 19 and Fig. 20, for the phase and attenuation constants:
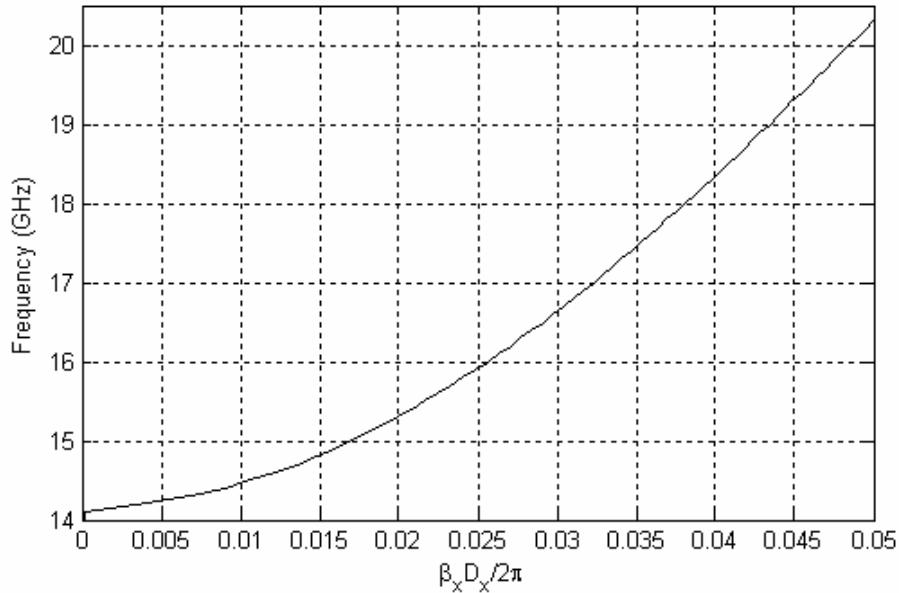

Fig. 19. Normalized leaky-wave phase ($\hat{\beta}$) constant as a function of frequency f for the relevant TE leaky mode of a LWA antenna.

Below the cut off frequency, there is a bandgap and hence, there is no propagation of this mode. Over cut off frequency, there is a passband, corresponding with the mode seen in Fig. 19, where wave propagates.
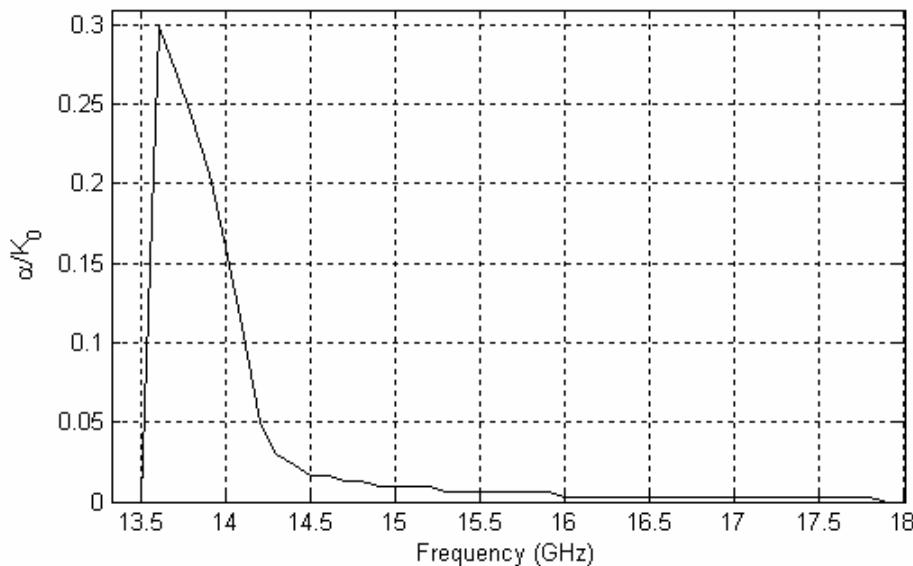

Fig. 20. Normalized leaky-wave attenuation ($\hat{\alpha}$) constant as a function of frequency f for the relevant TE leaky mode of a LWA antenna.

As it can be observed, below the cut off frequency, the value of α is very high due to the fact that for those frequencies there is a bandgap. Once reached the cut off, the attenuation constant decreases to normal values.

For the propagation constant, the results obtained in this project are very similar to the ones obtained in [16]. One more time it indicates that the Minimum Research Method has been verified. Nevertheless, these results were difficult to find due to the fact that in the Minimum Search method, the minimum that the program found for specific frequencies, was the minimum in the asymptote for the maximum value of the range of beta.
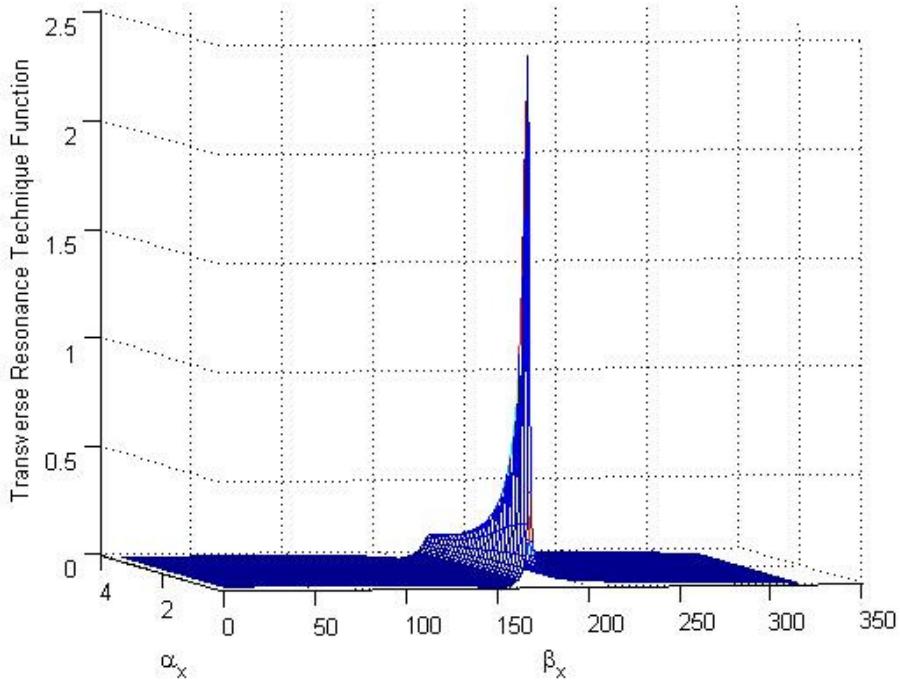

Fig. 21. Three dimensions plot. **Absolute value** of the Transverse Resonance Technique function, (17), against β and α for f=15.8GHz.

In order to solve this problem, once the structure in Fig. 21 was studied, it was necessary to add some code, in which there is a comparison with gradients of the function against β, for a fixed value of α. Once this first minimum has been located, the whole matrix which contains the absolute value of the function, is reduced to another matrix of β dimension equal to the result obtained as the first minimum plus a margin of error in the case in which there is variation over the total minimum as a function of α. In this way, we make sure that the solution given by the method is the first minimum found, not the one in the asymptote. Graphically, this problem is observed in the case of a specific frequency (f=15.8GHz) where the value of the Transverse Resonance Technique function is represented against all the range of β and α (Fig. 21), against α (for β=123, Fig. 22), and against β (for the first value of α, equal to zero, Fig. 23).
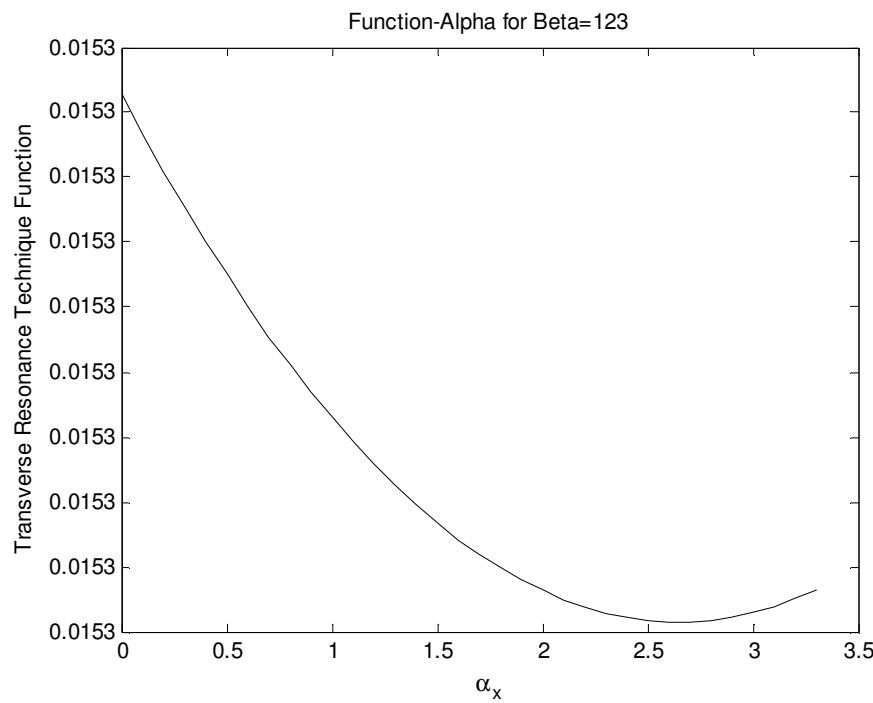
**Fig. 22.** **Absolute value** of the Transverse Resonance Technique function, (17), against α for f=15.8GHz and β=123.
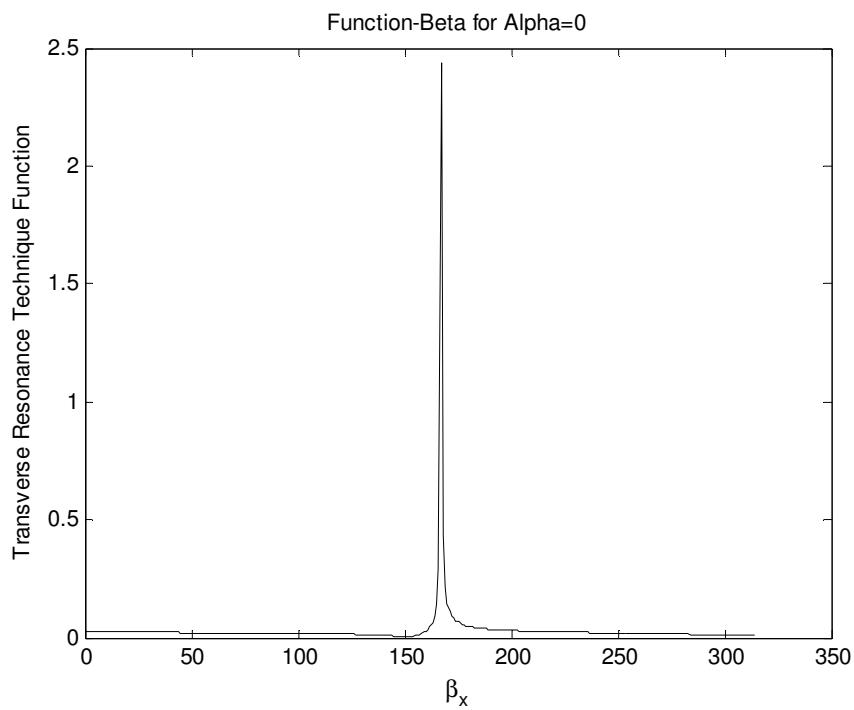
**Fig. 23.** **Absolute value** of the Transverse Resonance Technique function (17) against β for f=15.8GHz and α =0.

As it can be observed, the real minimum to find, is located between β=100 and β=150, but the program found the minimum in the asymptote for the maximum value of β given by the initial range.

b)   Antenna Performance.

One of the most important characteristics to study the behaviour of an antenna is its Radiation Pattern. "The Radiation Pattern of an antenna is a plot of the magnitude of the far/zone field strength versus position around the antenna, at a fixed distance from the antenna. Thus the radiation pattern can be plotted from the pattern functions $F_\theta(\theta,\phi)$ or $F_\phi(\theta,\phi)$, versus either the angle θ (for an elevation plane pattern) or the angle φ (for an azimuthally plane pattern). The choice of plotting either F_θ or F_ϕ is dependent on the polarization of the antenna. Since the pattern functions are proportional to voltage, the radial scale of the plot is computed as $20\log|F(\theta,\phi)|$; alternatively, the plot could be computed in terms of the radiation intensity as $10\log|U(\theta,\phi)|$. The pattern may exhibit several distinct lobes, with different maxima in different directions. The lobe having the maximum value is called the main beam, while those lobes at lower levels are called side lobes." [6]

In order to get the Radiation Pattern of the structure in Fig. 15, the Array Factor Approach Principle explained in [12] was used.

"A LW antenna can be considered a phased array antenna with inter-element spacing p in the limit where $p \to 0$, as illustrated in Fig. 24. While the phased array, Fig.24 a), is fed discretely at each nth element with a phase function $\xi_n(\theta_0)$ (θ_0 is the radiation angle) and usually a constant magnitude function $I_n = I_0(\forall n)$, the LW antenna, Fig. 24 b), is *fed* continuously solely at one end of the structure with a phase function $\xi(\theta_0)$ and an exponential magnitude function $I(x) = I_0\exp(-\alpha x)$, where α is the leakage factor.

In the case of metamaterials LW structures, the condition $p \to 0$, or more meaningfully $p/\lambda_g \to 0$, is satisfied by definition of an effective medium. The phase and magnitude functions can then be discretized as:

$$\xi_n = -(n-1)k_0 p \sin\theta_0 \text{ and } I_n = I_0 e^{-\alpha(n-1)p} \qquad (18)$$

Where p is the period of the structure and k_0 is the free space wavenumber. Since $p/\lambda_g \to 0$, each incremental period contribution will be equivalent to an isotropic radiator and the total radiation pattern $R(\theta)$ of the LW antenna can therefore be well approximated solely by the array factor function:

$$R(\theta) = AF(\theta) = \sum_{n=1}^{N} I_n e^{j(n-1)k_0 p \sin\theta + j\xi_n} \qquad (19)$$

Where N represents the number of unit cells constituting the structure (proportional to directivity), with ξ_n and I_n functions given by (18). In general, for periodic LW antennas the radiation angle in (18) is given by:

$$\theta_0 = \sin^{-1}\left[\frac{\beta(w)}{k_0}\right] \qquad (20)$$

Where $\beta(w)$ is the propagation constant in the direction of propagation." [12] and [13]
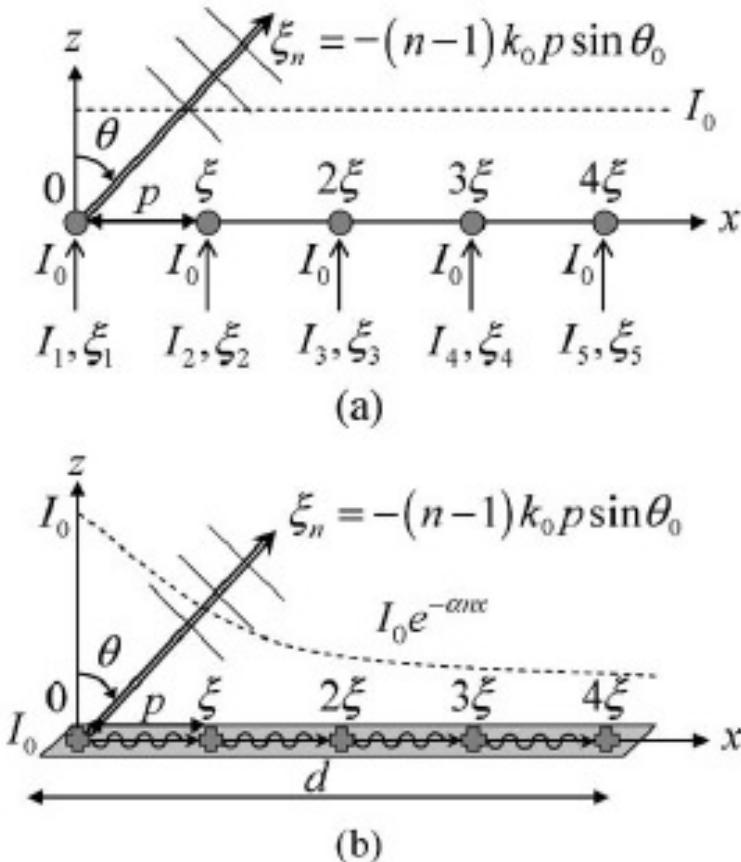

Fig. 24. Array factor approach principle. (a) Discrete configuration of a conventional phased array with elements interspacing p. (b) Continuous configuration of a periodic-structure leaky-wave antenna, with period p.[12]

For the structure in Fig. 15, the values of the dimensions indicated has been slightly changed due to the fact that it was necessary to work with a practical structure which was measured in other work. With these dimensions it has been possible to compare results. The new dimensions of the FSS unit cell are w_1=1.5 mm, w_2=0.5 mm, l_1=11 mm, l_2=10 mm, and S=h=11.1 mm. The dielectric support thickness is 1.13mm, and its permittivity $\varepsilon_r = 2.2$. The new values of α and β, which have been calculated in the same way as they were before, are shown in Fig. 25 and 26.
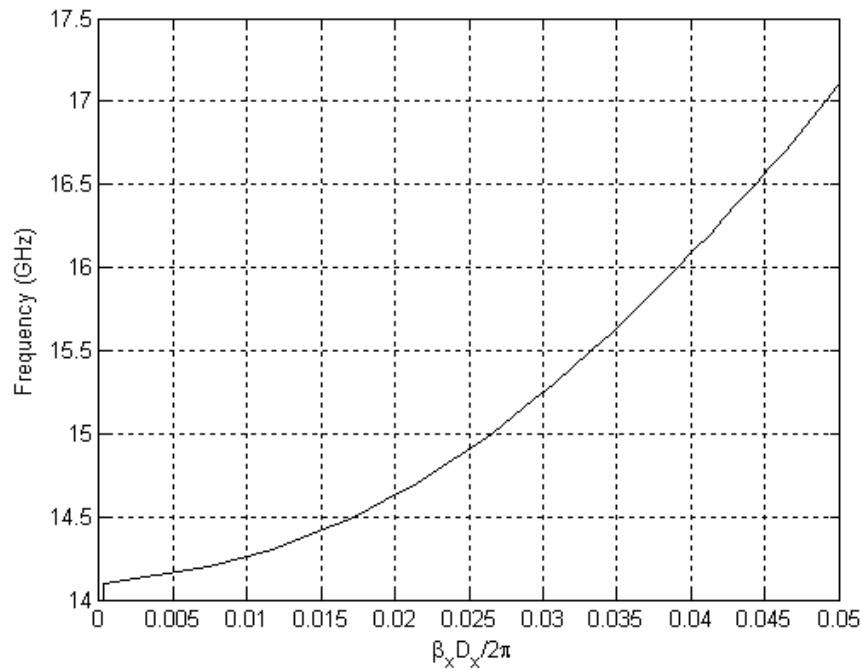
Fig. 25. Normalized leaky-wave phase ($\hat{\beta}$) constant as a function of frequency f for the relevant TE leaky mode of a LWA antenna. Practical structure, data: w_1=1.5 mm , w_2=0.5 mm, l_1=11 mm, l_2=10 mm and S=h=11.1 mm. The dielectric support thickness is 1.13 mm, and its permittivity $\varepsilon_r = 2.2$.
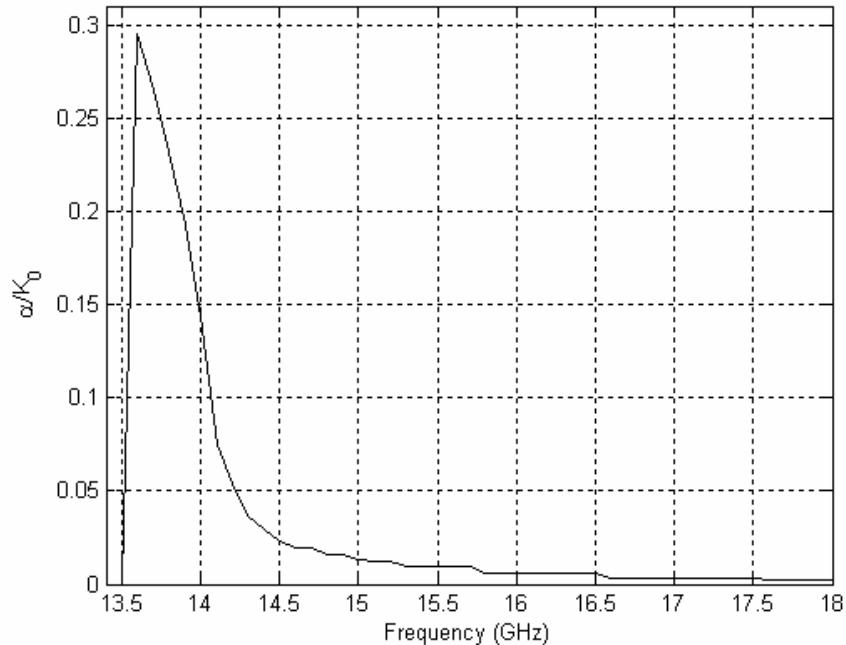

Fig. 26. Normalized leaky-wave attenuation ($\hat{\alpha}$) constant as a function of frequency f for the relevant TE leaky mode of a LWA antenna. Practical structure, data: w_1=1.5 mm , w_2=0.5 mm, l_1=11 mm, l_2=10 mm and S=h=11.1 mm. The dielectric support thickness is 1.13 mm, and its permittivity $\varepsilon_r = 2.2$.

The Radiation Pattern can be calculated for a specific frequency using the method explained above. Moreover, for a bi-directional leaky-wave antenna, such as the one shown in Fig.27, contribution from both poles k_p and $-k_p$ (being $k_p = \alpha_p + i\beta_p$) should be taken into account for the equation.
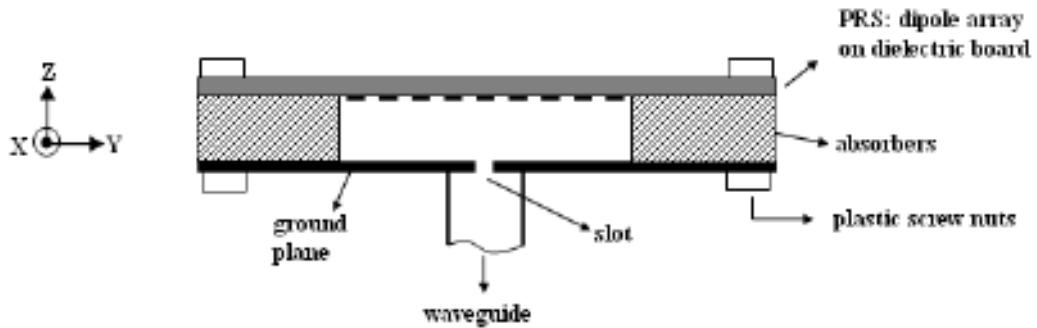

Fig. 27. Schematic diagram of a possible measured antenna. The thin dielectric board is placed to support the PRS and improve the accuracy of the measurements. [16]

In order to calculate the Radiation Pattern, for a bidirectional antenna, the result is the superposition of the contributions of (19) for positive and negative values of k_p but calculated for half of the total length L of the antenna. The absolute value of the solution in (19) for positive and negative k_p are multiplied and the product is divided by the maximum value of this product to be normalized, i.e. normalized by the value at the direction of maximum radiation. Finally, in order to get the Radiation Pattern, the results for different frequencies are plotted in logarithm scale. The following equation has been applied:

$$20\log\left(\frac{\left|F(\theta,\phi)\right|_{k_{positive}} \cdot \left|F(\theta,\phi)\right|_{k_{negative}}}{\max\left(\left|F(\theta,\phi)\right|_{k_{positive}} \cdot \left|F(\theta,\phi)\right|_{k_{negative}}\right)}\right) \qquad (21)$$

The plot corresponding with the Radiation Pattern calculated by using the method before explained for 15GHz, is shown in Fig. 28 and is compared with the measured results used in [16] for the same structure.
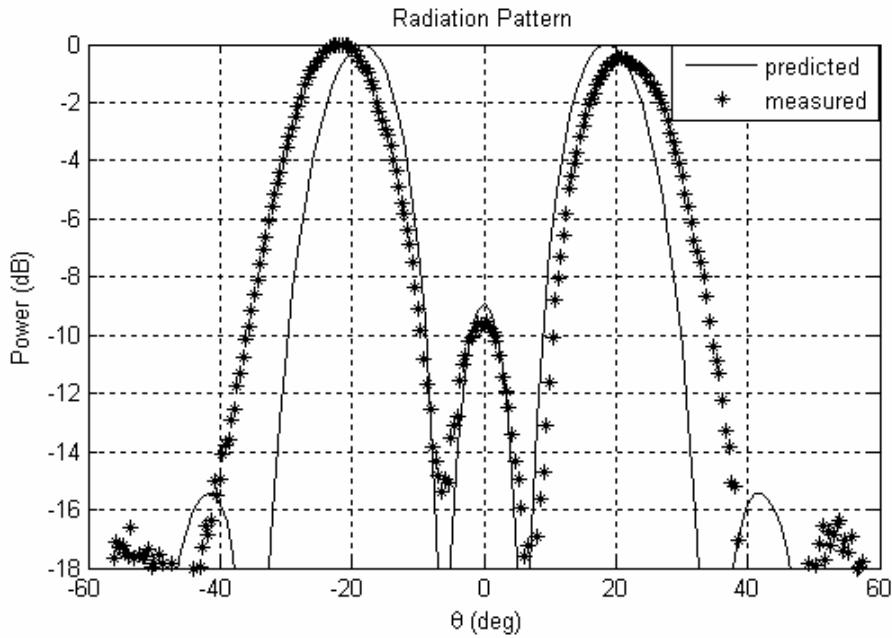
Fig. 28. Radiation Pattern calculated by the Minimum Search method and by using the measured data, for frequency 15GHz.

As it can be observed, the results obtained with the method implemented in this project and the ones measured are in very good agreement, one more time the method has been verified. Otherwise, some discrepancies can be also observed due to the limitations that experiments can have. They might be caused because of the diffraction effects at the edges of the copper and the absorber, or positioning and alignment errors, which can cause loss of symmetry in the pattern.

In order to study the behaviour of the antenna for different frequencies, some plots have been executed from the cut off frequency, where the radiation is broadside.

For 14.3 GHz, the Radiation Pattern is as follows:
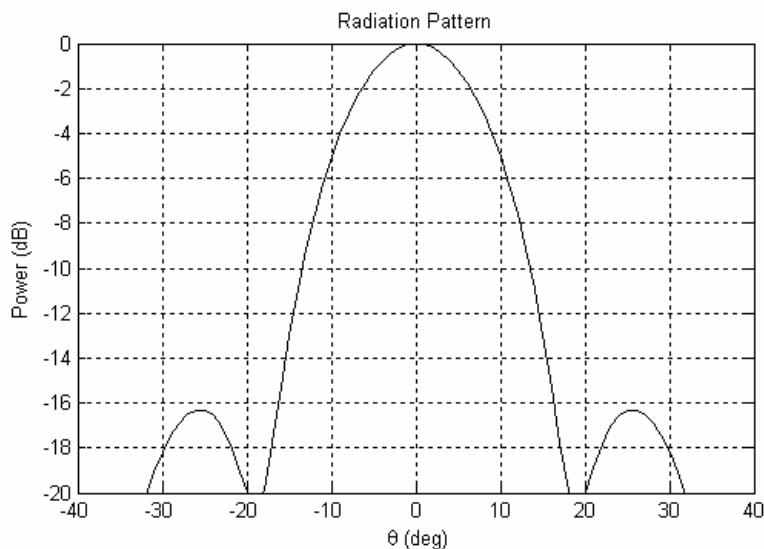
Fig. 29. Radiation Pattern calculated by the Minimum Search method for frequency 14.3 GHz.

62
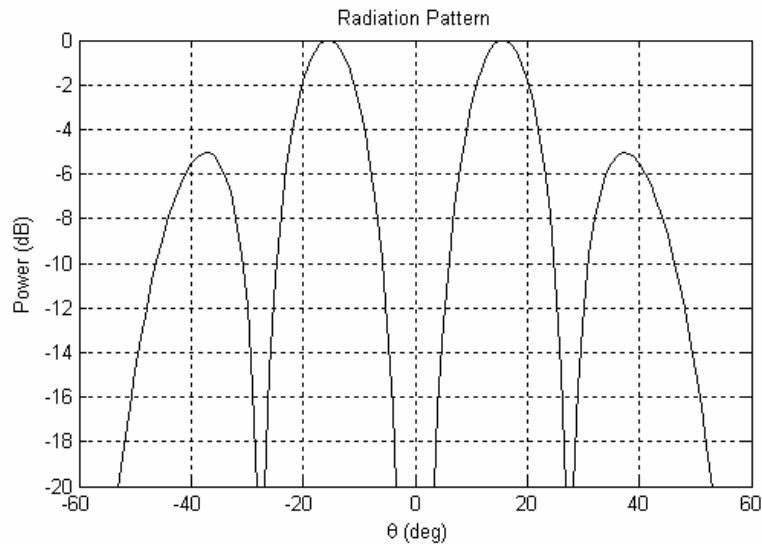
For 15.5 GHz:

Fig. 30. Radiation Pattern calculated by the Minimum Search method for frequency 15.5 GHz.

For 16.5 GHz:
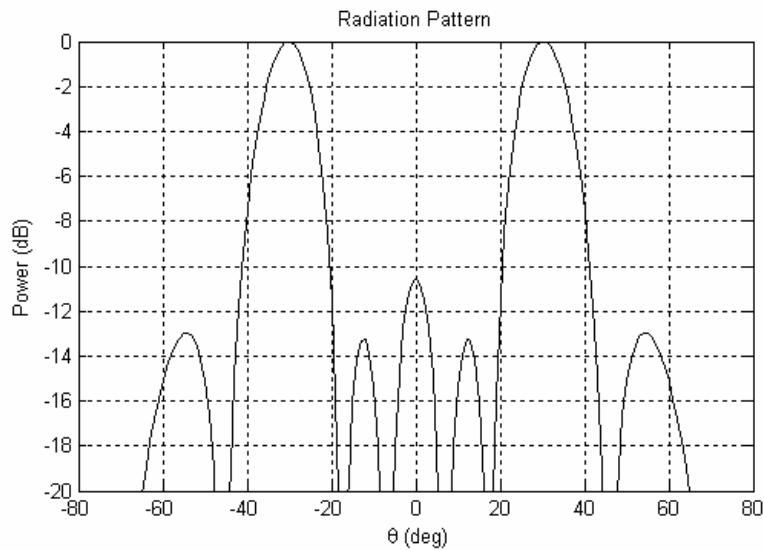
Fig. 31. Radiation Pattern calculated by the Minimum Search method for frequency 16.5 GHz.

As it has been observed, the angle of maximum radiation increase in the same way as does the frequency, appearing secondary lobes after the splitting up of the main lobe at broadside into two symmetric lobes, when the frequency is near the cut off.

III. CONCLUSIONS.

In this project, the application of the Transverse Resonance Technique for periodic structures has been studied, acting as Frequency Selective Surfaces, with the aim of calculating the Dispersion Diagrams and Radiation Patterns of these antennas. In order to solve the Transverse Resonance Technique function, a program in Matlab consisting of a minimum search method for both, minimum depending on one variable (Surface-Wave case) and minimum depending on two variables, in the complex plane (Leaky-Wave case), has been implemented, having been verified with the results of other papers and real measured values. The results obtained for this report were only achieved for TE surface-wave or leaky-wave modes (H-plane), but in the same way, and changing the equations of the impedances in the equivalent network, they could have also been obtained for TM modes (E-plane). Although for the TM modes, the results wouldn't have been so accurate due to the fact that the periodicity in E-plane is bigger, near the size $\lambda/2$ and for this reason, the surface can not be considered as a homogenous admittance, which is the basic theory in order to apply the equivalent network for the Transverse Resonance Technique.

As a possible extension of this project, a similar structure could be studied, but for more than one layer. In this case, it could be applied the same process followed in this project, by extending the equivalent network for an unit cell to a transmission line consisting in new admittances representing the layers of FSS. Nevertheless, instead of calculating the reflection coefficient by using the program in Fortran, it could be estimated by using the equations derived from a general theory for multimirror Fabry-Perot interferometers, where each layer would be represented by one mirror. [4]
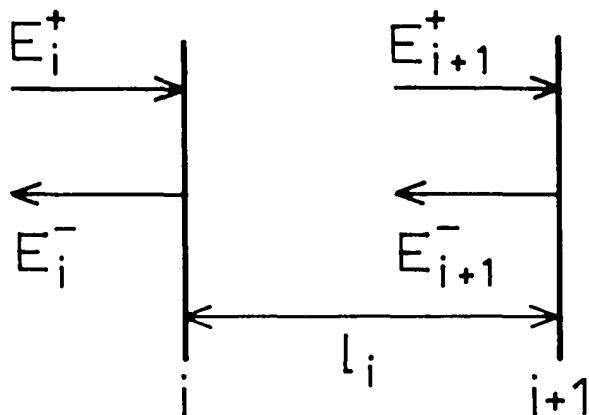
Fig. 32. The amplitudes at mirrors i and i+1 out of a stack of N mirrors. [4]

This theory could be explained supposing that N partially transmitting, plane parallel mirrors of zero thickness are sequentially numbered, i= 0…N. In Fig 32. there are two consecutives mirrors where the following parameters can be defined: E_i+ is the amplitude of the electric-field vector on the left-hand side of mirror i for a wave front propagating to the right; E_i - is the amplitude on the left-hand side of mirror i for a wave front travelling to

the left; r_i and t_j are the amplitude reflection and transmission coefficients for mirror i; the distance from mirror i to mirror (i +1) is L_i; however, it is better to use a phase length $\varphi_i = 2\pi L_i/\lambda$. All amplitudes implicitly assume the superposition of all multiple reflected beams.

The negative sign for r_i must be taken into account for beams incident upon the left-hand side and upon the right-hand side of mirror i, as determined by Stokes's law. So for two mirrors i and (i + 1) and assuming that there are no losses, the E fields equations are expressed as:

$$E_{i+1}^+ \exp(-i\phi_i) = t_i E_i^+ + r_i E_{i+1}^- \exp(+i\phi) \qquad (22)$$

$$E_i^- = -r_i E_i^+ + t_i E_{i+1}^- \exp(+i\phi_i) \qquad (23)$$

Where $r_i = E_i^+ \big/ E_i^-$ and $t_i = E_{i+1}^+ \big/ E_i^+$.

Eliminating E_i+ and knowing that without losses $r^2+t^2=1$, the following expression for a series of N plane parallel partially transmitting mirrors is obtained:

$$
\begin{pmatrix} E_1^+ \\ E_1^- \end{pmatrix} = \frac{1}{t_1 t_2 .. t_{N-1}} \begin{bmatrix} \exp(-i\phi_1) & -r_1 \exp(i\phi_1) \\ -r_1 \exp(i\phi_1) & \exp(i\phi_1) \end{bmatrix} \times \begin{bmatrix} \exp(-i\phi_2) & -r_2 \exp(-i\phi_2) \\ -r_2 \exp(-i\phi_2) & \exp(-i\phi_2) \end{bmatrix} \times ...
$$
$$
\times \begin{bmatrix} \exp(-i\phi_{N-1}) & -r_{N-1} \exp(-i\phi_{N-1}) \\ -r_{N-1} \exp(-i\phi_{N-1}) & \exp(-i\phi_{N-1}) \end{bmatrix} = \begin{pmatrix} E_N^+ \\ E_N^- \end{pmatrix} \qquad (24)
$$

To conclude, some definitions must be done. The amplitude transmission of such a stack of N mirrors can be expressed as follows:

$$t = t_1 t_2 ... t_N \big/ (A - r_N B) \qquad (25)$$

Being A and B some of the coefficients of the resulting matrix of (24). T can also be defined as the intensity transmission:

$$T = tt^* \qquad (26)$$

This last parameter is commonly used in plots against the phase length in order to represent the total transmission response of the structure.

In following work, it would be interesting to study different structures based on several layers of FSS using this theory as a possible improvement of the analysis of this kind of antennas. Moreover, it would be also interesting to study more in depth the method applied in the calculation of minimum over two variables, for example in the case of Leaky-Wave, through intelligent techniques over complex poles searches.[18]

To conclude, this technique provides a fast and accurate method to know the behaviour of an antenna before its manufacture, which, in general, would save time and cost, such important factors in any organization. Otherwise, a more complex and slowly process like the modal analysis should be applied over the whole structure, increasing drastically the computing cost with the number of layers. For this reason, the application of the method implemented in this project, offers an easy solution for the characterization of this kind of Frequency Selective Surfaces Antennas.

ACKNOWLEDGMENT

REFERENCES

[1] Raj Mittra, Chi H. Chan, and Tom Cwik, "Techniques for Analyzing Frequency Selective Surfaces- A Review", IEEE, vol. 76, no. 12, Dec. 1988.

[2] S.B. Savia and E.A.Parker, "Equivalent circuit model for superdense linear dipole FSS", IEEE Proc.-Microw. Antennas Propag., Vol. 150, no.1, Feb. 2003.

[3] G. Goussetis, A.P. Feresidis, G. K. Palikaras, M.Kitra, and J.C. Vardaxoglou, "Miniaturization of electromagnetic band gap structures for mobile applications", Radio Science, Vol. 40, 2005.

[4] Herman van de Stadt and Johan M. Muller, "Multimirror Fabry-Perot interferometers", J. Opt. Soc. Am. A, Vol. 2, no. 8, August 1985.

[5] G. Goussetis, A. P. Feresidis, and J.C. Vardaxoglou, " Tailoring the AMC and EBG Characteristics of Periodic Metallic Arrays Printed on Grounded Dielectric Substrate", IEEE Trans. Antennas and Propagation, Nov. 2004, submitted for publication.

[6] Pozar, D., *Microwave Engineering*, Addison/Wesley, Boston, Mass, 1998,2nd Ed.

[7] Collin, R. E., *Foundations for Microwave Engineering*, McGraw-Hill, 1992.

[8] J. C. Vardaxoglou, *Frequency Selective Surfaces: Analysis and Design*, John Wiley, Hoboken, N. J., 1997.

[9] Marcuvitz. N.: "Waveguide handbook" (Dover Publications Inc. New York, 1965), pp.280/285.

[10] Archer. M.J: "Wave reactance of thin planar strip gratings". Int. J. Electron, 1985, 58, (2), pp. 187/230.

[11] A.P. Feresidis and J.C. Vardoxoglou: "High gain planar antenna using optimized partially reflective surfaces", IEEE Proc-Microw. Antennas Propag., Vol. 148, No. 6, December 2001.

[12] C. Caloz and T. Itoh: "Array Factor Approach of Leaky/Wave Antennas and Application to 1/D/2-D Composite Right/Left-Handed (CRLH) Structures." IEEE Microwave and wireless components letters, Vol.14, No. 6, June 2004.

[13] C.A. Balanis, *Antenna Theory*, 2nd ed. New York: Wiley, 1997.

[14] A.A. Oliner 'Leaky wave Antennas' Chapter 10, *Antenna Engineering Handbook,* 3ª ed. McGrawHill, 1993.

[15] G. Lovat, P. Burghignoli and D.R. Jackson, " Fundamental Properties and Optimization of Broadside Radiation From Uniform Leaky-Wave Antennas ", IEEE Trans. Antennas Propag., vol. 54, No. 5, May. 2006.

[16] P. Kosmas, A. P. Feresidis and G. Goussetis, "Periodic FDTD analysis of a 2-D leaky-wave planar antenna based on dipole frequency selective surfaces", submitted to IEEE Trans. Antennas Propag., March, 2006.

[17] T. Zhao, D. R. Jackson, J. T. Williams and A. A. Oliner, "General formulas for 2-D leaky-wave antennas", IEEE Trans. Antennas Propag., vol. 53, No. 11, pp. 3525-3533, Nov. 2005.

[18] Gómez.J.L, G.Goussetis, A.A. Melcon, "Robust and systematic algorithm to assist in the complex-poles search task for stub-loaded leaky-wave antennas", submitted for publication to IEEE Trans. Antennas and Propagation.

[19] Gómez.J.L, Pascual. J., A.A. Melcon, "Efficient full-wave analysis method of leaky-wave modes in periodically loaded dielectric waveguides with application to backward-to-forward frequency-scannable antennas and metamaterials", International journal of numerical modelling: Electronic Networks, Devices and Fields. Int. J. Numer. Model. 2006; 19:173-193. Published online in Wiley InterScience (www.interscience.wiley.com). DOI: 10.1002/jnm.605

APPENDICES

APPENDIX I: *PHAROSRCONDIP* PROGRAM

PHAROSRcondip program was implemented in Fortran by using the Modal Analysis explained in the Introduction, in the section B. 2). This analysis is based on the Moment Method (MoM) and it is applied in structures of one or two layers of the patched periodic structures consisted of dipoles.

The Program generates an output.txt file from an input file with information about incident fields, the transmission and the reflection coefficient of the structure simulated.

The following text is an example of an input file (the one used for the Structure 3):

```
00.00001 00.0001 00.001 ! theta phi wmega

1.0 1.0 1.0 ! er1 er0 er2

0.00 0.0 0.00 ! tand

0.00001 0.0 0.0 ! S1 Sair S2

1.0 14.5 90.0 00.0 !Dx Dy alpha alpha1

14.0 0.5 ! l(y) w(x)

17 0.0 0.0 ! Floquet modes, shiftx shifty

1.0 14.5 90.0 00.0 !Dx Dy alpha alpha1

14.0 0.5 ! l(y) w(x)

17 0.0 0.0 !FM2 DSX(w) DSY(l)

0.1 0.1 22  !fstart fstep fstop
```

Where *l* and *w* refers to the dimensions of the dipoles and D_x and D_y the periodicity in the corresponding axis, and S and ε_r are the height and relative permittivity of the dielectric respectively. For Theta and Phi equal to 0 the incidence is broadside and all the dimensions are in millimetres, angles in degrees and frequency in GHz.

The structure is represented in the output file and is shown as follows:

```
   Z0                  Z1                 Z2                 Z3

   *                    I                  *                  I
   *                    I                  *                  I
   *    ERD1 =  1.000   I   ERDA =  1.000  *   ERD2 =  1.000  I
   *                    I                  *                  I
   *    LTN1 =   .000   I   LTNA =   .000  *   LTN2 =   .000  I
   *                    I                  *                  I
   *                    I                  *                  I
   *    S1 =   .0000100 I   SEP=  .0000000 *   S2 =  .0000000 I
   *                    I                  *                  I
   *                    I                  *                  I
```

Where the arrays are located at $z=z_0$ and $z=z_2$, and $z=z_1$ and $z=z_3$ are boundaries between possible dielectrics.

APPENDIX II: MATHEMATICAL DEVELOPMENTS

A. ABCD Parameters

ABCD transmission parameter is ideal for cascaded 2-port system due to the fact that it only requires knowledge of 2-by-2 matrix multiplication and it is simple, almost direct calculation for forward or reverse mixed voltage or current transfer functions. The ABCD matrix is defined for a two-port network in terms of the total voltages and currents as shown in Fig. 33. Input port 1 and Output port 2 voltages and currents are related through the parameters: A,B,C and D in matrix form as follow:

$$\begin{bmatrix} V_1 \\ I_1 \end{bmatrix} = \begin{bmatrix} A & B \\ C & D \end{bmatrix} \cdot \begin{bmatrix} V_2 \\ I_2 \end{bmatrix} \qquad \Longrightarrow \qquad \begin{array}{l} V_1 = AV_2 + BI_2 \\ I_1 = CV_2 + DI_2 \end{array}.$$
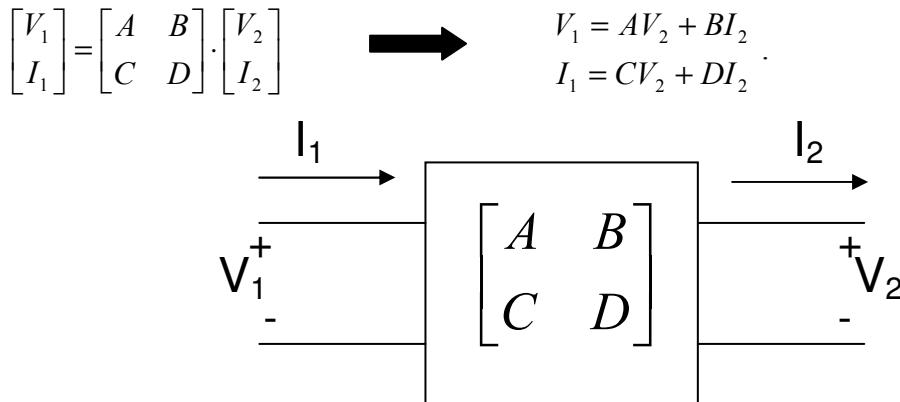

Fig. 33. Two-port network transmission matrix for ABCD parameters.

According to this definition, the current I_2 flows out of port 2, because for the analysis when dealing with ABCD matrices in a cascade network, I_2 is considered as flowing out of port 2, i.e., into the adjacent network [6].

A and C are derived by "open-circuited" port 2, and B and D are derived by "short-circuited" port 2 as shown below.

$$A = \left.\frac{V_1}{V_2}\right|_{I_2=0}, \quad B = \left.\frac{V_1}{I_2}\right|_{V_2=0}, \quad C = \left.\frac{I_1}{V_2}\right|_{I_2=0} \quad \text{and} \quad D = \left.\frac{I_1}{I_2}\right|_{V_2=0}.$$

1) Admittance:

The ABCD-parameters for a shunt arm with admittance Y represented in Fig. 34 are calculated.
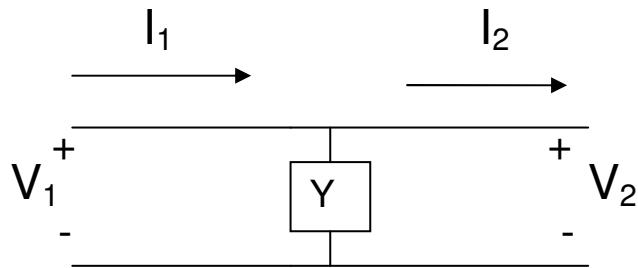

Fig. 34. Two-port network for a shunt arm with admittance Y.

As $V_1 = V_2$, then the ABCD Parameters are the following:

$$A = \left.\frac{V_1}{V_2}\right|_{I_2=0} = 1, \quad B = \left.\frac{V_1}{I_2}\right|_{V_2=0} = 0, \quad C = \left.\frac{I_1}{V_2}\right|_{I_2=0} = \frac{V_1/_{1/Y}}{V_1} = Y \quad \text{and} \quad D = \left.\frac{I_1}{I_2}\right|_{V_2=0} = 1 \quad \text{(no}$$

current flows through Y)

2) Transmission Line:

The two-port network corresponding with a transmission line is shown in Fig. 32.
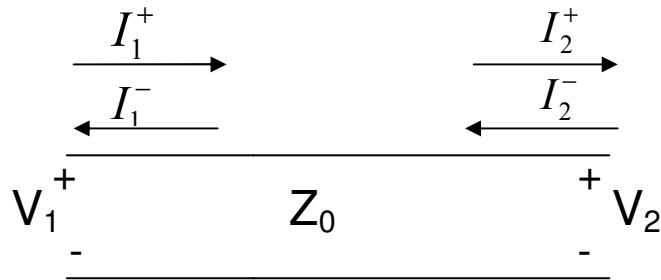
Fig. 35. Two-port network for a transmission line.

For being in a transmission line, equations for V_1 and I_1 are expressed as follow:

$$\begin{array}{l} V_1 = V_2^+ e^{j\beta l} + V_2^- e^{-j\beta l} \\ I_1 = I_2^+ e^{j\beta l} - I_2^- e^{-j\beta l} \end{array}, \text{ where } I_2^+ = \frac{V_2^+}{Z_0} \text{ and } I_2^- = \frac{V_2^-}{Z_0}.$$

Then the ABCD Parameters are the following:

• $A = \left.\frac{V_1}{V_2}\right|_{\substack{I_2=0 \\ Z_L=\infty \\ \rho=1}} = \frac{V_2^+ e^{j\beta l} + V_2^- e^{-j\beta l}}{V_2^+ + V_2^-} = \frac{V_2^+ \left(e^{j\beta l} + e^{-j\beta l}\right)}{2V_2^+} = \frac{2\cos\beta l}{2} = \cos\beta l, \text{ where } \rho = \frac{V_2^-}{V_2^+},$

and as we are in a case of open-circuited, its value is 1, what means that the reflected voltage is in phase with the incident voltage and the reflected current has opposite polarization to the incident current (see pag. 61 from [6] for more details).

• $B = \left.\frac{V_1}{I_2}\right|_{\substack{V_2=0 \\ Z_L=0 \\ \rho=-1}} = \frac{V_2^+ e^{j\beta l} + V_2^- e^{-j\beta l}}{I_2^+ - I_2^-} = \frac{V_2^+ \left(e^{j\beta l} - e^{-j\beta l}\right)}{\dfrac{V_2^+}{Z_0}(1+1)} = jZ_0 \sin\beta l, \text{ where } \rho = \frac{V_2^-}{V_2^+}, \text{ and as}$

we are in a case of short-circuited, its value is -1, what means that the reflected voltage is not in phase with the incident voltage and the reflected current has the same polarization that the incident current (see pp. 60 from [6] for more details).

$$\bullet \ C = \left.\frac{I_1}{V_2}\right|_{\substack{I_2=0 \\ Z_L=\infty \\ \rho=1}} = \frac{I_2^+ e^{j\beta l} - I_2^- e^{-j\beta l}}{V_2^+ + V_2^-} = \frac{\dfrac{V_2^+}{Z_0} e^{j\beta l} - \dfrac{V_2^-}{Z_0} e^{-j\beta l}}{V_2^+(1+1)} = \frac{\dfrac{V_2^+}{Z_0}\left(e^{j\beta l} - e^{-j\beta l}\right)}{V_2^+(1+1)} = \frac{j\sin\beta l}{Z_0} = jY_0 \sin\beta l$$

, (open-circuited case, $\rho = \dfrac{V_2^-}{V_2^+} = 1$).

$$\bullet \ D = \left.\frac{I_1}{I_2}\right|_{\substack{V_2=0 \\ Z_L=0 \\ \rho=-1}} = \frac{I_2^+ e^{j\beta l} - I_2^- e^{-j\beta l}}{I_2^+ - I_2^-} = \frac{I_2^+\left(e^{j\beta l} + e^{-j\beta l}\right)}{I_2^+(1+1)} = \cos\beta l , \qquad \text{(short-circuited} \quad \text{case,}$$

$\rho = \dfrac{V_2^-}{V_2^+} = -1$).

B. *Analytical development for structure 1*

As it has been indicated in the Applications section of this report, the Transverse Resonance Technique function for structure 1 has the following expression:

$Y_s + 2 \cdot Y_0 = 0$ (I)

Where:

$Y = \dfrac{1}{Z}$ (in general), $Z_s = jwL + \dfrac{1}{jwC}$, and $Z_0^{TE} = \dfrac{K_0 \cdot \eta_0}{K_z} = \dfrac{w \cdot \mu_0}{K_z}$.

Therefore, the equation (I) is expressed as follows:

$$\frac{jwC}{1-w^2 LC} + \frac{2k_z}{w\mu_0} = 0 \rightarrow \frac{2k_z}{w\mu_0} = -\frac{jwC}{1-w^2 LC} = -\frac{jwC}{1-\left(\dfrac{w}{w_0}\right)^2} , \ \text{where } w_0 = 1/\sqrt{LC} , \ \rightarrow$$

$$\rightarrow k_z = -\frac{jw^2 C\mu_0}{2\left(1-\left(\dfrac{w}{w_0}\right)^2\right)} = \frac{jwCk_0\eta_0}{2\left(1-\left(\dfrac{w}{w_0}\right)^2\right)} \ \text{(II)}$$

In order to get an analytical solution for the propagation constant in the y axis direction (supposing no propagation in x axis), (7) is applied, and substituting (II) in this equation, the expression for k_y is as follows:

$$k_y = \sqrt{k_0^2 - k_z^2} = \sqrt{k_0 + \frac{w^2 C^2 k_0^2 \eta_0^2}{4\left(1 - \left(\dfrac{w}{w_0}\right)^2\right)^2}} = k_0 \sqrt{1 + 0.25 \left[\frac{wC\eta_0}{1 - \left(\dfrac{w}{w_0}\right)^2}\right]^2} \; .$$

Knowing that the expression for k_0 is: $k_0 = \dfrac{2\pi}{\lambda} = \dfrac{2\pi f}{c} = \dfrac{w}{c}$, the final expression for k_y is as follows:

$$k_y^{TE} = \frac{w}{c} \sqrt{1 + 0.25 \left[\frac{wC\eta_0}{1 - \left(\dfrac{w}{w_0}\right)^2}\right]^2}$$

Where η_0 represents the free space wave impedance and $w_0 = 1/\sqrt{LC}$, is the resonant frequency of the series LC circuit representing the array.

APPENDIX III: MATLAB CODES

C. Surface Waves

1) Structure 1:

- Code for the analytical solution:

```matlab
%Frequency rate
f=linspace(0.1,4e9,200);

%Data
Zo=376.730313461;
L=2e-9;
Cthin=0.41e-12;
Cthick=13.28e-12;
Dthin=12e-3;
Dthick=14e-3;
c=3e8;
wothin=1/sqrt(L*Cthin);
wothick=1/sqrt(L*Cthick);
w=2*pi*f;

%Propagation constant
for i=1:length(w)
Ktethin(i)=(w(i)/c)*sqrt(1+0.25*((Zo*w(i)*Cthin)/(1-
(w(i)/wothin)^2))^2);
Ktethick(i)=(w(i)/c)*sqrt(1+0.25*((Zo*w(i)*Cthick)/(1-
(w(i)/wothick)^2))^2);
end

Ktethinnorm=Ktethin*(Dthin/pi);
Ktethicknorm=Ktethick*(Dthick/pi);

jthin=find(Ktethinnorm>=0.5);  %We only plot until kte=pi/D o
ktenorm=1 because of the periodicity
jthick=find(Ktethicknorm>=0.5);

%Plots
figure(1),
title('f-k diagram');
plot(Ktethinnorm(1:jthin(1)),f(1:jthin(1)),'k'); hold on;
plot(Ktethicknorm(1:jthick(1)),f(1:jthick(1)),'k--'); hold
off;
grid on;
xlabel('Normalised Propagation Constant kte
(pi/D)');ylabel('Frequency (GHz)');
legend('thin','thick');
```

- Code for the Minimum Search Method:

```
%Frequency rate
f=linspace(0.1e9,4e9,20000);
epsr=2.2;
c=3e8;
K0=2*pi*f/c;
w=2*pi*f;
mu0=4*pi*1e-7;
L=2e-9;
Cthin=0.41e-12;
Cthick=13.28e-12;
Dthin=12e-3;
Dthick=14e-3;

%Propagation constant
Kytethin=K0(1)+1:1:pi/Dthin;
Kytethick=K0(1)+1:1:pi/Dthick;

for q=1:length(f)

  functhin=j*w(q)*Cthin/(1-(w(q)^2)*L*Cthin)-2*sqrt(K0(q)^2-
Kytethin.^2)./(w(q)*mu0);
  functhick=j*w(q)*Cthick/(1-(w(q)^2)*L*Cthick)-
2*sqrt(K0(q)^2-Kytethick.^2)./(w(q)*mu0);


KyteMinimumthin(q)=Kytethin(find(abs(functhin)==min(abs(funct
hin))));

KyteMinimumthick(q)=Kytethick(find(abs(functhick)==min(abs(fu
ncthick))));

end
KyteMinimumNormthin=KyteMinimumthin.*Dthin/pi;
KyteMinimumNormthick=KyteMinimumthick.*Dthick/pi;


jthin=find(KyteMinimumNormthin>=0.5);  %We only plot until
kte=pi/D o ktenorm=1 because of the periodicity
jthick=find(KyteMinimumNormthick>=0.5);

%Plots
figure (1),
plot(KyteMinimumNormthin(1:jthin(1)),f(1:jthin(1)),'k'); hold
on;
plot(KyteMinimumNormthick(1:jthick(1)),f(1:jthick(1)),'k--');
hold off;
grid on;
xlabel('Normalised Propagation Constant Kyte
(pi/D)');ylabel('Frequency (GHz)');
legend('thin','thick');
```

D. Leaky Waves

1) Structure 2:

```matlab
%Frequency rate
f=linspace(20.3e9,21e9,180);

%Data
epsr=2.2;
c=3e8;
K0=2*pi*f/c;
w=2*pi*f;
mu0=4*pi*1e-7;
mur=1;
S=5e-3;
eps0=8.8542e-12;
eta0=sqrt(mu0/eps0);
Bs=20/eta0;

for q=1:length(f)

    clear func;
    beta=0:1:0.3*K0(q);
    alfa=beta;
    [Re,Im]=meshgrid(beta,alfa);

    Kyte=Re-j*Im;

    term1=(sqrt(K0(q)^2-Kyte.^2))./(K0(q)*eta0);
    Kzdielec=sqrt(epsr*mur*K0(q)^2-Kyte.^2);
    term2=-j*(Kzdielec).*cot(S*(Kzdielec))./(K0(q)*mur*eta0);
    term3=j*Bs;

    func=term1+term2+term3;

    [fila, columna]=find(abs(func)==min(min(abs(func))));

    KyteRealMinimum(q)=beta(columna);
    KyteImagMinimum(q)=alfa(fila);


    KyteRealMinimumNorm(q)=KyteRealMinimum(q)/K0(q);
    KyteImagMinimumNorm(q)=KyteImagMinimum(q)/K0(q);

end

%Plots
figure (1),
plot(f*1e-9,KyteRealMinimumNorm,'k');grid on;hold on;
plot(f*1e-9,KyteImagMinimumNorm,'k--');
title('Frequency-Kyte');
ylabel('Kyte');xlabel('Frequency (GHz)');
legend('Beta','Alfa');
```

2) Structure 3

```matlab
%Frequency rate
Array=spcread(5);%Matrix obtained from Fortran program.
%Frequency rate
f=Array(:,1)*1e9;

%% ---------DATA-----------------------------------------
--------------
c=3e8;
K0=2*pi*f/c;
w=2*pi*f;
mu0=4*pi*1e-7;
mur=1;
S= 11.1e-3;
eps0=8.8542e-12;
eta0=sqrt(mu0/eps0);
Dx=1.5e-3;
longx=8.5e-2;

%% ---------IMPLEMENTATION-------------------------------
---------------
for q=1:length(f)

    clear func;
    beta=0:1:350;
    alfa=0:1:(3e-1)*K0(q);
    [B,A]=meshgrid(beta,alfa);

    Kyte=B-j*A;

    %We look for the reflexion coefficient for f(q).
    % module (column4) and phase (column5)of Rxs. The
argument must be in rad

Rxs=Array(q,4)*cos(Array(q,5)*pi/180)+j*Array(q,4)*sin(Array(
q,5)*pi/180);

    %TE
    term1=(sqrt((K0(q))^2-Kyte.^2))./(K0(q)*eta0);
    term2=-j*term1.*cot(S*sqrt((K0(q))^2-Kyte.^2));
    term3=-2*Rxs.*term1./(1+Rxs);

    func=term1+term2+term3;

    %We do that to get the minimum value for Beta in the last
position of the row
    k=1;
    while (abs(func(1,k+1))<=abs(func(1,k)))

        k=k+1;
    end

    %We delete the zeros in func2.
```

```matlab
    func2=func(:,1:k+1);

    [fila, columna]=find(abs(func2)==min(min(abs(func2))));

    KyteRealMinimum(q)=beta(columna);
    KyteImagMinimum(q)=alfa(fila);


    KyteRealMinimumNorm(q)=KyteRealMinimum(q)*Dx/(2*pi);
    KyteImagMinimumNorm(q)=KyteImagMinimum(q)/K0(q);

end

%% --------RADIATION PATTERN------------------------------
--------------

fRP=find(Array(:,1)==15); %We look for the frequency to study
the radiation pattern
theta=[-90:90];

thetarad=theta*pi/180;

N=floor(longx/(Dx))+1;
n=[0:floor((N-1)/2)];
[Ang,Element]=meshgrid(thetarad,n);

q=0; %For 1D Leaky wave antenna.
theta0N=asin(-KyteRealMinimum(fRP)/K0(fRP));
theta0P=asin(KyteRealMinimum(fRP)/K0(fRP));
epsnN=-(Element).*K0(fRP)*Dx.*sin(theta0N);
epsnP=-(Element).*K0(fRP)*Dx.*sin(theta0P);
I0=1;
InN=I0*exp(-KyteImagMinimum(fRP)*(Element)*Dx);
InP=I0*exp(-KyteImagMinimum(fRP)*(Element)*Dx);



MatrixRN=InN.*exp(j*(Element)*K0(fRP)*Dx.*sin(Ang)+j.*epsnN);
MatrixRP=InP.*exp(j*(Element)*K0(fRP)*Dx.*sin(Ang)+j.*epsnP);

RN=sum(MatrixRN);%We obtain a row with the sum of each column
(for each theta)
RP=sum(MatrixRP);

producto=abs(RP).*abs(RN);

maxproducto=max(producto);

RPTotaldB=20*log10(producto/maxproducto);

%% --------PLOTS-------------------------------------------
--------------

figure (1),
plot(KyteRealMinimumNorm,f*1e-9,'k');grid on;
```

```matlab
xlabel(' \beta_xD_x/2\pi');ylabel('Frequency (GHz)');

figure (2),
plot(f*1e-9,KyteImagMinimumNorm,'k');grid on;
ylabel(' \alpha/K_0');xlabel('Frequency (GHz)');


%We load the measured data for the corresponding frequency
load DIPA15.dat;

maxlog=max(DIPA15(:,2));%It is obtained in order to normalize
the data.
long=length(DIPA15(:,2));
relleno=repmat(DIPA15(1,2),6,1);
DIPM=[relleno;DIPA15(1:long-6,2)];

figure (3),
plot(theta,RPTotaldB,'k');grid on;hold on;
plot(DIPA15(:,1),DIPM-maxlog,'k*');hold off;
title('Radiation Pattern');
xlabel(' \theta (deg)');ylabel('Power (dB)');
legend('predicted','measured');

figure (4),
plot(theta,20*log10(abs(RP)),'k');grid on;hold on;
plot(theta,20*log10(abs(RN)),'r');hold off;
title('Radiation Pattern');
xlabel(' \theta (deg)');ylabel('Power (dB)');
```